Int J Adv Manuf Technol (2017) 89:333–354
DOI 10.1007/s00170-016-9077-3

ORIGINAL ARTICLE

Comparative assessment of two ceramic cutting tools on surface roughness in hard turning of AISI H11 steel: including 2D and 3D surface topography

A. Khellaf[1,2] · H. Aouici[2,3] · S. Smaiah[4] · S. Boutabba[1] · M. A. Yallese[2] · M. Elbah[2,3]

Received: 21 February 2016 / Accepted: 15 June 2016 / Published online: 1 July 2016

Abstract This paper presents a comparison of surface roughness between both ceramic cutting tools namely, TiN coated mixed ceramic CC6050 and uncoated mixed ceramic CC650 when machining hardened hot work steel X38CrMoV5-1 [AISI H11] treated at 50 HRC. A mathematical model, relating surface roughness criteria and main factors such as cutting radius, cutting speed, feed rate, and depth of cut, was developed using response surface methodology (RSM) and its adequacy was checked by regression analysis. The effect of cutting parameters on surface roughness is evaluated and the optimum cutting conditions to minimize the surface roughness are determined. A multiple linear models have been established between the cutting parameters and the surface roughness using response surface methodology. The experimental results reveal that the most significant machining parameter for surface roughness is the feed followed by cutting radius. Also the determined optimal conditions really reduce the surface roughness on the machining of AISI H11 steels within the ranges of parameters studied. In addition, excellent surface roughness was obtained in hard turning using CC650 tools. The coated ceramic tools had no advantage over CC650 from the point of view of surface roughness.

Keywords Hard turning · AISI H11 steel · Ceramic · Surface roughness · ANOVA · RSM

Nomenclature

Vc	Cutting speed (m/min)
HRC	Rockwell hardness
f	Feed rate (mm/rev)
ANOVA	Analysis of variance
ap	Depth of cut (mm)
RSM	Response surface methodology
r	Cutting radius (mm)
DF	Degrees of freedom
Ra	Arithmetic mean roughness (μm)
Seq SS	Sequential sum of squares
Rt	Total roughness (μm)
Adj MS	Adjusted mean squares
Fc	Tangential force (N)
Cont. %	Contribution ratio (%)
HT	Hard turning
R^2	Coefficient of determination (%).

1 Introduction

Nowadays, hard turning (HT) is the most interesting topic in industrial production and scientific research [3]. It has been applied in many cases in producing bearings, gears, cams, shafts, axels, and other power transmission and mechanical parts since the early 1980s. Hard turning operations involve the cutting of materials with hardness from 45 to 68 HRC [10]. As a consequence, the tool materials are hard. Some of the

✉ A. Khellaf
khellafahmed@hotmail.fr; khellafahmedgmp@gmail.com

1 Département de Génie Mécanique, Laboratoire de Mécanique Appliquée des Nouveaux Matériaux (LMANM), Université 08 Mai 1945, BP 401, Guelma 24000, Algeria

2 Département de Génie Mécanique, Laboratoire Mécanique et Structure (LMS), Université 08 Mai 1945, BP 401, Guelma 24000, Algeria

3 Ecole Nationale Supérieure de Technologie (ENST), Dergana, Algeria

4 Ecole Nationale Polytechnique (ENP), El Harrache, Algeria

main tool materials include the following: ceramics, cubic boron nitride (CBN) and coated CBN, polycrystalline cubic boron nitride (PCBN), polycrystalline diamond (PCD), or tungsten carbide (WC) coated with titanium nitride (TiN) [27].

Unfortunately, extreme tribological conditions developed at dry severe friction and high tool–chip and work–flank interface temperatures tend towards the acceleration of tool wear, and as a consequence a relatively fast deterioration of surface finish and dimensional and shape accuracy. Today, research activities in HT sector are primarily focused on CBN tool wear (the material predominantly used in the cutting tool) [21, 28, 31]. Oppositely, new data on turning hardened AISI D3 and 100Cr6 bearing steels using ceramic tools are reported in ref. [4]. In general, ceramic tools have attracted the attention of researchers and some works can be highlighted. With the development of ceramic tool materials, they are more and more widely used in the field of metal cutting because their mechanical properties and cutting performances have been greatly improved. They have been used in many applications due to their improved properties like good thermal shock resistance, good high-temperature strength, creep resistance, low density, high hardness and wear resistance, electrical resistively, and better chemical resistance [11].

The surface roughness describes the geometry of the surface to be machined and combined with surface texture. The formation of surface roughness mechanism is very complicated and mainly depends on machining process [1, 33]. Hence, it is very difficult to determine the surface roughness through analytical equations. The surface finish can be characterized by two main parameters, arithmetic mean roughness (*Ra*) and total roughness (*Rt*). Geometric models have been proposed to estimate these parameters and are given as [6, 29] where are based only on the geometry of the tool (radius nose) and feed rate.

$$Ra = \frac{f^2}{32r} \tag{1}$$

$$Rt = \frac{f^2}{8r} \tag{2}$$

where f is the feed rate (mm/rev) and r is the tool nose radius (mm).

The work completed by the scientific community [19, 32], when reporting the performance of ceramic tools in the machining of various hard materials, has shown that the surface roughness depends on cutting parameters (cutting speed and feed rate) and tool's geometry. Lima et al. [23] evaluated the changes of *Ra* surface roughness on 58 HRC AISI D2 cold work steel parts in terms of *VB* wear indicator in turning, using mixed alumina inserts at the cutting speeds of 80, 150, and 220 m/min and three feeds of 0.05, 0.1, and 0.15 mm/rev and 1 mm depth of cut. For example, after 5 min turning test ($Vc = 150$ m/min, $f = 0.1$ mm/rev), the *Ra* of 0.5 μm corresponded to the wear land width of $VB = 0.10$ mm, and after other 10 min when wear progressed to 0.18 mm the relevant *Ra* value increased to 0.58 μm. In another study, Grzesik and Wanat [20] investigated the surface finish generated in hard turning of quenched alloy steel (60 HRC) using conventional and wiper ceramic inserts. They determined that surfaces produced by wiper tools contained blunt peaks with distinctly smaller slopes resulting in better bearing properties. In order to determine machinability rates and surface roughness, tool wear and cutting force components were measured. A new optimization approach called the Multivariate Robust Parameter Design (MRPD) was applied by Paiva et al. [25] with the target of minimal surface roughness during hard turning of AISI 52100 steel with coated mixed ceramic inserts. In a recent study, Bouacha et al. [7] used the ANOVA to evaluate the significance of cutting parameters on cutting force and surface roughness obtained in hard turning of AISI 52100 steel with CBN tool. The effect of tool material (ceramic and CBN) and cutting parameters (speed, feed rate, and depth of cut) on surface roughness was studied by Darwish [9] using two-level factorial designs (23). He further demonstrated a favorable effect for ceramic inserts on surface roughness when compared with CBN inserts at both high and low feed rates. Fnides et al. [18] conducted the experimental study to determine the statistical models of surface roughness criteria in turning hardened AISI H11 (X38CrMoV5-1) steel (50 HRC) with mixed ceramic tool. Mathematical models, based on Minitab software, were elaborated in order to express the influence degree of each cutting mode on surface roughness. The results indicate that feed rate is the dominant factor affecting surface roughness, followed by cutting speed. However, the effect of the depth of cut is not very important. Recently, Elbah et al. [16] compared the values of surface roughness obtained with wiper and conventional ceramic inserts during hard turning of AISI 4140 steel. They disclosed that the improved surface quality is achieved with wiper geometry.

In order to get good surface quality and dimensional properties, it is necessary to employ optimization techniques to find optimal cutting parameters and theoretical models to do predictions. Taguchi and response surface methodologies can be conveniently used for these purposes. Suresh [30] used the response surface method and genetic algorithm to predict the surface roughness and to optimize the process parameters. In a present study, Dureja et al. [14] applied the response surface methodology (RSM) to investigate the effect of cutting parameters on flank wear and surface roughness in hard turning of AISI H11 steel with a coated mixed ceramic tool. The study indicated that the flank wear is influenced principally by feed rate, depth of cut, and workpiece hardness. Jenn-Tsong et al.

[22] developed the RSM model using the CCD in the hard turning which uses uncoated Al_2O_3/TiC mixed ceramic tool for flank wear and surface roughness. Flank wear was influenced principally by the cutting speed and the interaction effect of feed rate with tool's nose radius. The cutting speed and the tool corner radius affected surface roughness significantly.

The current study investigates the influence of cutting parameters (cutting radius (*r*, mm), cutting speed (*Vc*, m/min), feed rate (*f*, mm/rev), and depth of cut (*ap*, mm)) in relation with surface roughness (*Ra*) on machinability. The processing conditions are turning of hardened hot work steel (AISI H11) with two different ceramic tools (CC6050 coated with TiN and CC650 conventional) using RSM and ANOVA. This last is a computational technique that enables the estimation of relative contributions of each of the control factors to the overall measured response. In this work, the significant parameters will be used to develop mathematical models using RSM. The RSM is a collection of mathematical and statistical techniques that are useful for the modeling and analysis of problems in which interest response is influenced by several variables and the objective is to optimize the response.

2 Experimental conditions and procedures

2.1 Material, workpiece, and tool

Turning experiments were performed in dry conditions using lathe, which is made by TOS TRENCIN company; mode SN 40C with 6.6 kW spindle power. The cutting conditions for finish hard turning under higher parametric condition are shown in Table 2.

The workpiece material used for the experiments is grade AISI H11 steel, hot work steel bars with dimensions of 400 mm length and 75 mm in diameter, which is popularly used in hot form pressing. Its resistance to high temperature, its tenacity, its aptitude for polishing, and its impact resistance thermal properties enable it to answer to the most severe requests in hot dieing and molds under pressure [17]. Its chemical composition is given in Table 1. It is hardened to 50 HRC (quenching at 1020 °C followed by oil tempering at 250 °C). Its hardness was measured by a digital durometer DM2D.

Table 1 Chemical composition of AISI H11 steel

Composition	(Wt%)
C	0.35
Cr	5.26
Mo	1.19
V	0.50
Si	1.01
Mn	0.32
S	0.002
P	0.016
Other components	1.042
Fe	90.31

A tool holder and insert geometry, having the ISO designation: PSBNR2525K12 and SNGA120408T01020, respectively, were employed with tool geometry as follows: $\chi = 75°$; $\alpha = 6°$; $\gamma = -6°$; $\lambda = -6°$. Tool flank wear was inspected several times during the tool's life, using an optical microscope (Visual Machine 250). Tool life was considered ended when the flank wear reached $VB = 0.30$ mm. At the end of the tool's life, worn inserts were examined in a scanning electron microscope (SEM).

The measurements of the surface roughness (*Ra* and *Rt*) for each cutting condition were obtained from a Surftest 201 Mitutoyo roughness meter. It consists of a diamond point (probe) with a 5-μm radius and moves linearly on the working surface. The length examined is 4.0 mm with a basic span of 0.8 mm. The measured values of *Ra* are within the range 0.05 to 40 μm while for *Rt* they lay between 0.3 and 160 μm. Roughness measurements were directly obtained without disassembling the turned part in order to reduce uncertainties due to resumption operations.

In addition, four measurements were made using a three-dimensional (3D) surface topography with optical platform of metrology modular Altisurf 500. The three-dimensional topographic maps of the machined surfaces were produced using the interferometry technique (Fig. 1). 3D data were also taken along the pitch-surface generator, the shape was removed, and then parameters were calculated with the Gaussian filter (cut-off was 0.8 mm).

2.2 Design of experiment

(a) Orthogonal array

The surface roughness has been measured after the straight turning operation. In this study, a factorial design was used to identify the main effects of four factors [cutting radius (*r*, mm), cutting speed (*Vc*, m/min), feed rate (*f*, mm/rev), and depth of cut (*ap*, mm)] on the responses namely arithmetic mean roughness (*Ra*) and total roughness (*Rt*) when using two cutting tools: uncoated mixed ceramic (CC650) and TiN coated mixed ceramic (CC6050).

The planning of experiments was based on Taguchi's L_{36} orthogonal array, with factors ("A", "B", "C" and "D") and three levels for ("B," "C," "D") and two levels for "A." In the matrix shown in Table 3, the three levels are represented by "−1," "0," and "+1," where "−1" is the lowest level and "+1" is the highest. For each experiment, 36

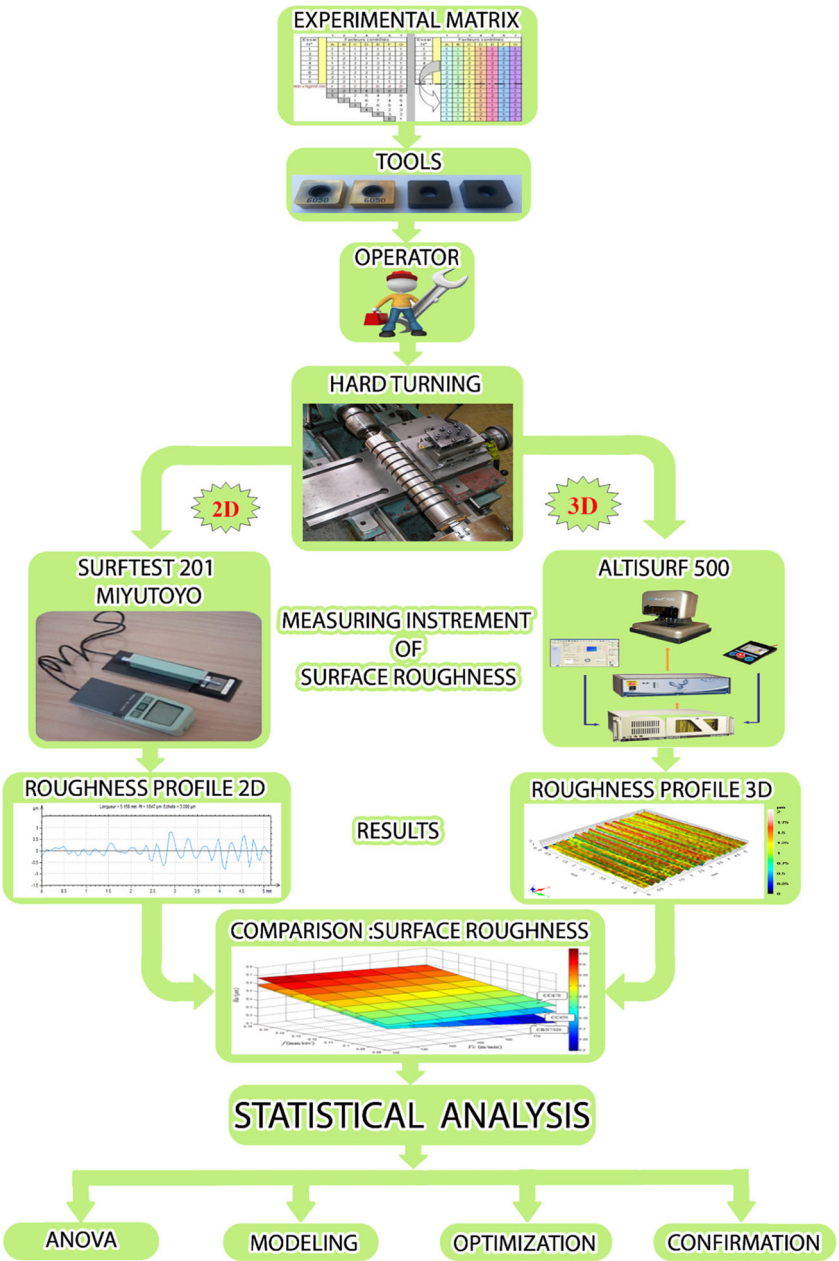

Fig. 1 Illustration of measured surface roughness criteria

machining trials were carried out. The considered factors are given in Table 3. Their levels were chosen according to the cutting tool specifications (Table 2).

(b) Response surface methodology

The RSM is a procedure used to determine the relationship between the independent process parameters with the desired response and exploring the effect of these parameters on responses. The present investigation has been planned in the following steps:

(a) Identify the important factors, which influence the surface roughness on the machining of AISI H11 steels;
(b) Find the upper and lower limits of the factors identified;
(c) Develop the experimental design matrix using design of experiments;
(d) Conduct the experiments as per the design matrix;
(e) Empirical modeling to approximate the relationship (i.e., the response surface) between responses and factors;
(f) Analyze the results using ANOVA;
(g) Optimize the chosen factor levels to attain minimum surface roughness;
(h) Confirm experiments and verify the predicted performance characteristics.

Table 2 Cutting parameters and their levels for turning

Symbol	Control factor	Unit	Symbol of factors	Levels		
				Level 1	Level 2	Level 3
ap	Depth of cut	mm	D	0.10	0.30	0.50
f	Feed rate	mm/rev	C	0.08	0.14	0.20
Vc	Cutting speed	m/min	B	100	150	200
r	Cutting radius	mm	A	0.80	1.20	

(c) Development of the mathematical model

The response function representing the surface roughness criteria can be expressed as:

$$Y = \varphi(A, B, C, D) \tag{3}$$

where Y = response (surface roughness criteria).

The multiple linear polynomial (regression) equation used to represent the response surface for k factors is given by the relation:

$$Y = b_0 + \sum_{i=1}^{k} b_i X_i + \sum_{i,j}^{k} b_{ij} X_i X_j \tag{4}$$

where b_0 is the free term of the regression equation, the coefficients b_1, b_2,…b_k are linear terms and b_{12}, b_{13},…b_{k-1},b_k are the interaction terms. *Xi* represents input parameters (*r*, *Vc*, *f*, and *ap*). The outputs (*Ra* and *Rt*) are also called the response factors. The experimental plan and the result of trials are reported in Table 3. Based on the plan of Taguchi $2^1 \times 3^3$ full factorial design, a total of 36 tests were carried out.

For four factors, the selected polynomial could be expressed as:

$$Y = b_0 + b_1 r + b_2 Vc + b_3 f + b_4 ap + b_5 r \times Vc + b_6 r \times f + b_7 r \times ap + b_8 Vc \times f + b_9 Vc \times ap + b_{10} f \times ap \tag{5}$$

2.3 Analysis of variance (ANOVA)

The analysis of variance has been applied to check the adequacy of the developed machinability models. ANOVA can be useful to determine the influence of any given input parameters from a series of experimental results by the design of experiments for machining process and it can be used to interpret experimental data. The obtained results are analyzed using Design Expert V8, a statistical analysis software which is widely used in many engineering applications. The ANOVA table consists of sum of squares and degrees of freedom. The mean square is the ratio of sum of squares to degrees of freedom and F value is the ratio of mean square to the mean square of the experimental error [8]. The statistical significance of the fitted multiple linear models is evaluated by the P values and F values of ANOVA.

In ANOVA table, P value is the probability (ranging from 0 to 1) that the results observed in a study (or results more extreme) could have occurred by chance.

- If P value 0.05, the parameter is significant;
- If P value 0.05, the parameter is insignificant.

The important coefficient R^2 measures the percentage of data variation that is explained by the regression equation. The adjusted R^2 value is particularly useful when comparing models with different number of terms. When R^2 approaches to unity, the response model fits the actual data effectively.

3 Results and discussion

The results of the machining trials performed as per the experimental plan are shown in Table 3. These results were entered into the Design Expert software for further analysis following the steps outlined in Section 2.2b. The Table 3 shows all values of surface roughness criteria (*Ra* and *Rt*) when using two cutting tools namely, coated CC6050 and uncoated CC650 ceramic tools. The surface roughness criteria were obtained in the range of (0.18–1.51 and 1.33–7.96) μm and (0.20–1.36 and 0.69–6.77) μm, respectively, for CC6050 and CC650.

3.1 Statistical analysis

Tables 4 and 5 show ANOVA results, respectively, for *Ra* and *Rt* for both ceramic cutting tools (CC650 and CC6050). This analysis was out for a 5 % significance level, i.e., for 95 % confidence level. In addition to degree of freedom, mean of squares (MS), sum of squares (SS), F value, and probability (Prob.) associated to each factor level were presented. The last column of tables shows the factor contribution (percentage; Cont. %) on the total variation, indicating the degree of influence on the result.

Table 4 shows the results of ANOVA model for surface roughness parameter namely arithmetic mean roughness (*Ra*) of coated ceramic (CC6050) and uncoated ceramic (CC650) tools. From the analysis of Table 4, it can be apparent seen that the model is significant and the feed rate (*f*, mm/rev) is the most important factor affecting *Ra*. Its contribution is (72.245 and 89.953) %. This is because its increase generates helicoid furrows, the result of tool shape and helicoid movement tool–workpiece. These furrows become deeper and broader when the feed rate increases. However, a qualitative comparison can be made; for example, Dilbag and Venkateswara [13] found that the feed rate and the radius nose are the important factors affecting surface roughness. The next

Table 3 L_{36} ($2^1 \times 3^3$) orthogonal array, experimental results for surface roughness

Test no.	Machining parameters				Surface roughness			
					CC650		CC6050	
	r (mm)	*Vc* (m/min)	*f* (mm/rev)	*ap* (mm)	*Ra* (μm)	*Rt* (μm)	*Ra* (μm)	*Rt* (μm)
1	0.8	100	0.08	0.1	0.67	3.65	0.39	2.61
2	0.8	150	0.14	0.3	0.63	3.23	0.76	4.40
3	0.8	200	0.20	0.5	1.14	5.60	1.48	7.40
4	0.8	100	0.08	0.1	0.66	3.30	0.37	2.56
5	0.8	150	0.14	0.3	0.61	3.96	0.80	4.76
6	0.8	200	0.20	0.5	1.36	6.77	1.51	7.01
7	0.8	100	0.08	0.3	0.29	1.82	0.36	2.67
8	0.8	150	0.14	0.5	0.58	3.27	0.73	4.34
9	0.8	200	0.20	0.1	1.30	6.26	1.40	6.38
10	0.8	100	0.08	0.5	0.36	3.46	0.30	2.38
11	0.8	150	0.14	0.1	0.67	3.59	0.73	3.76
12	0.8	200	0.20	0.3	1.10	5.25	1.50	7.96
13	0.8	100	0.14	0.5	0.63	3.88	0.71	4.21
14	0.8	150	0.20	0.1	1.24	6.31	1.24	5.70
15	0.8	200	0.08	0.3	0.31	2.16	0.33	2.46
16	0.8	100	0.14	0.5	0.68	3.57	0.67	3.88
17	0.8	150	0.20	0.1	1.28	6.70	1.26	6.68
18	0.8	200	0.08	0.3	0.27	2.25	0.24	1.65
19	1.2	100	0.14	0.1	0.63	3.41	0.54	3.12
20	1.2	150	0.20	0.3	0.79	4.36	1.10	6.13
21	1.2	200	0.08	0.5	0.30	1.81	0.26	1.77
22	1.2	100	0.14	0.3	0.41	2.69	0.59	3.22
23	1.2	150	0.20	0.5	0.52	2.88	1.12	6.28
24	1.2	200	0.08	0.1	0.26	1.87	0.18	1.33
25	1.2	100	0.20	0.3	0.82	4.50	1.07	5.41
26	1.2	150	0.08	0.5	0.33	2.45	0.24	1.66
27	1.2	200	0.14	0.1	0.51	2.68	0.50	3.38
28	1.2	100	0.20	0.3	0.92	4.58	1.03	5.99
29	1.2	150	0.08	0.5	0.26	2.19	0.30	2.47
30	1.2	200	0.14	0.1	0.54	2.86	0.46	2.93
31	1.2	100	0.20	0.5	0.66	0.69	1.08	6.17
32	1.2	150	0.08	0.1	0.29	2.03	0.30	2.00
33	1.2	200	0.14	0.3	0.46	3.05	0.42	2.63
34	1.2	100	0.20	0.1	1.13	4.98	1.16	6.13
35	1.2	150	0.08	0.3	0.20	1.48	0.28	2.09
36	1.2	200	0.14	0.5	0.33	2.21	0.42	3.48

largest factor influencing *Ra* is cutting radius (*r*, mm) with (12.105 and 4.898) % contribution, for CC650 and CC6050 tools, respectively. Other model terms can be considered not significant. Another important coefficient R^2 in the resulting ANOVA table is defined as the ratio of the explained variation to the total variation and it is a measure of the degree of fit. When R^2 approaches to unity, the better response model fits the actual data. The value of R^2 calculated in Tables 4 and 5 for these models are over 0.91 for both ceramic tools CC650 and CC6050 and reasonably close to unity, which is acceptable. It denotes that about 95 % of the variability in the data is explained by these models. It also confirms that these models provide an excellent explanation of the relationship between the independent X_i factors and the response Y_i.

The results given by ANOVA analysis of surface roughness *Rt* for both ceramic cutting tools are presented in Table 5. It is observed that the parameters, feed rate (Cont. = 55.339 % and Cont. = 93.084 %) and cutting radius (Cont. = 15.660 % and

Table 4 Analysis of variance for *Ra*

Source	SS	DF	MS	*F* value	Prob.	Cont. %	Remarks
(a) CC650							
Model	3.701743	10	0.37017431	26.32226	<0.0001		Significant
A-*r*, mm	0.317911	1	0.31791178	22.60599	< 0.0001	12.105	Significant
B-*Vc*, m/min	0.023762	1	0.02376211	1.689670	0.2055	0.905	Insignificant
C-*f*, mm/rev	1.897396	1	1.89739643	134.9195	< 0.0001	72.245	Significant
D-*ap*, mm	0.171704	1	0.17170417	12.20949	0.0018	6.538	Significant
AB	0.000672	1	0.00067277	0.04783	0.8286	0.026	Insignificant
AC	0.087192	1	0.08719213	6.200036	0.0198	3.320	Significant
AD	0.005410	1	0.00541017	0.384705	0.5407	0.206	Insignificant
BC	0.008830	1	0.00883093	0.62794	0.4356	0.336	Insignificant
BD	0.092884	1	0.09288452	6.604809	0.0165	3.537	Significant
CD	0.020574	1	0.02057459	1.463013	0.2378	0.783	Insignificant
Residual	0.35157	25	0.01406316				
Lack of fit	0.31637	16	0.01977369	5,055773	0.0091		Significant
Pure error	0.0352	9	0.00391111				
Cor total	4.053322	35				100	
SD = 0.12					$R^2 = 0.9133$		
Mean = 0.64					R^2 Adjusted = 0.8786		
Coefficient of variation = 18.45					R^2 Predicted = 0.8091		
Predicted residual error of sum of squares (PRESS) = 0.77					Adequate precision = 16.701		
(b) CC6050							
Model	6.038464	10	0.60384643	76.23911	<0.0001		Significant
A-*r*, mm	0.179108	1	0.17910833	22.61346	<0.0001	4.898	Significant
B-*Vc*, m/min	0.002216	1	0.00221681	0.279885	0.6014	0.061	Insignificant
C-*f*, mm/rev	3.289100	1	3.28910046	415.2680	<0.0001	89.953	Significant
D-*ap*, mm	0.003504	1	0.00350417	0.442421	0.5120	0.096	Insignificant
AB	0.083535	1	0.08353521	10.54680	0.0033	2.285	Significant
AC	0.051658	1	0.05165824	6.522152	0.0171	1.413	Significant
AD	0.003139	1	0.00313962	0.396395	0.5347	0.086	Insignificant
BC	0.030636	1	0.03063683	3.868077	0.0604	0.838	Insignificant
BD	0.005318	1	0.0053184	0.671478	0.4203	0.145	Insignificant
CD	0.008257	1	0.00825726	1.042527	0.3170	0.226	Insignificant
Residual	0.198010	25	0.00792043				
Lack of fit	0.188110	16	0.01175692	10.68810	0.0005		Significant
Pure error	0.009900	9	0.0011				
Cor total	6.236475	35				100	
SD = 0.089					$R^2 = 0.9682$		
Mean = 0.72					R^2 Adjusted = 0.9555		
Coefficient of variation = 12.40					R^2 Predicted = 0.9242		
Predicted residual error of sum of squares (PRESS) = 0.47					Adequate precision = 27.899		

Cont. = 3.223 %) have great influence on the total roughness (*Rt*) of CC650 and CC6050, respectively, especially the feed rate. Earlier, Aouici et al. [2] observed that the effect of the feed rate was so notable on surface roughness criteria. Other model terms and interaction can be considered not significant.

The correlation coefficients R^2 of about (0.8624 and 0.9488) are considered good. It represents the proportion of variation in the response which is explained by the model. The "Pred. R^2" of (0.6860 and 0.8932) is in reasonable agreement with the "Adj. R^2" of (0.8074 and 0.9283) for both cutting ceramic tools, respectively.

One of the methods used to analyze data for process optimization is the use of Pareto ANOVA (Fig. 2). Pareto ANOVA is a simplified ANOVA method which uses Pareto principles. It is a quick and easy method to analyze results of parameter design. It does not require an ANOVA table and therefore does

Table 5 Analysis of variance for *Rt*

Source	SS	DF	MS	*F* value	Prob.	Cont. %	Remarks
(a) CC650							
Model	70.90744	10	7.09074415	15.67095	<0.0001		Significant
A-*r*, mm	8.152613	1	8.15261377	18.01774	0.0003	15.660	Significant
B-*Vc*, m/min	0.058907	1	0.05890714	0.130188	0.7213	0.113	Insignificant
C-*f*, mm/rev	28.80886	1	28.8088632	63.66924	<0.0001	55.339	Significant
D-*ap*, mm	3.270816	1	3.27081666	7.228693	0.0126	6.283	Significant
AB	0.048931	1	0.04893190	0.108142	0.7450	0.094	Insignificant
AC	1.390497	1	1.39049737	3.073079	0.0919	2.671	Insignificant
AD	1.651184	1	1.65118431	3.649212	0.0676	3.172	Insignificant
BC	0.929685	1	0.92968558	2.054658	0.1641	1.786	Insignificant
BD	3.579892	1	3.57989214	7.911767	0.0094	6.877	Significant
CD	4.167336	1	4.16733631	9.210053	0.0056	8.005	Significant
Residual	11.31192	25	0.45247689				
Lack of fit	10.11842	16	0.63240139	4.768841	0.0112		Significant
Pure error	1.193500	9	0.13261111				
Cor total	82.21936	35					
SD = 0.67					$R^2 = 0.8624$		
Mean = 3.49					R^2 Adjusted = 0.8074		
Coefficient of variation = 19.26					R^2 Predicted = 0.6860		
Predicted residual error of sum of squares (PRESS) = 25.81					Adequate precision = 13.794		
(b) CC6050							
Model	120.11806	10	12.0118064	46.285163	<0.0001		Significant
A-*r*, mm	2.4681083	1	2.46810833	9.5103761	0.0049	3.223	Significant
B-*Vc*, m/min	0.0238445	1	0.02384454	0.0918803	0.7643	0.031	Insignificant
C-*f*, mm/rev	71.274847	1	71.2748471	274.64378	<0.0001	93.084	Significant
D-*ap*, mm	0.8325375	1	0.8325375	3.2080215	0.0854	1.087	Insignificant
AB	0.7523151	1	0.75231516	2.8989003	0.1010	0.983	Insignificant
AC	0.0894116	1	0.08941166	0.3445304	0.5625	0.117	Insignificant
AD	0.0898803	1	0.0898803	0.3463362	0.5615	0.117	Insignificant
BC	0.7154013	1	0.71540132	2.7566600	0.1093	0.934	Insignificant
BD	0.1112695	1	0.1112695	0.4287554	0.5186	0.145	Insignificant
CD	0.2127386	1	0.2127386	0.8197468	0.3739	0.278	Insignificant
Residual	6.4879356	25	0.25951742				
Lack of fit	4.8856356	16	0.30535223	1.7151407	0.2075		Significant
Pure error	1.6023	9	0.17803333				
Cor total	126.606	35				100	
SD = 0.51					$R^2 = 0.9488$		
Mean = 4.08					R^2 Adjusted = 0.9283		
Coefficient of variation = 12.48					R^2 Predicted = 0.8932		
Predicted residual error of sum of squares (PRESS) = 13.52					Adequate precision = 22.233		

not use *F* tests. The following graphs are the Pareto ANOVA results of surface roughness criteria for CC650 and CC6050, respectively.

The Pareto ANOVA analysis technique, which requires less knowledge about ANOVA method which makes it suitable for engineers and industrial practitioners, has been performed. Effects are standardized (*F* value) for a better comparison. Standardized values in Fig. 2 are obtained by dividing the effect of each factor by the error on the estimated value of the corresponding factor. The more standardized the effect, the higher the factor considered influence. If the *F* values of the table are greater than 4.24, the effects are significant. By cons, if the *F* values of the table are less than 4.24, the effects are not significant. The confidence interval chosen is 95 %.

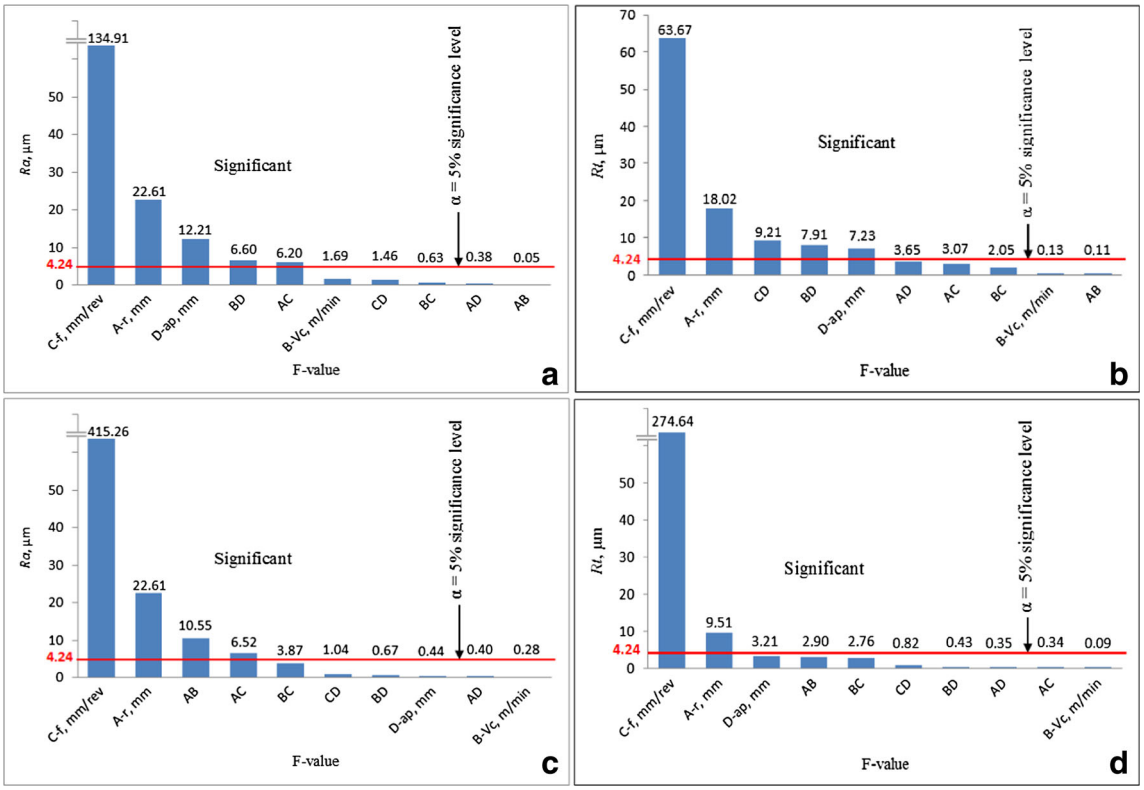

Fig. 2 Graphs of Pareto, for effect cutting parameters on surface roughness criteria

3.2 Mathematical modeling

The correlation between the effective factors (cutting speed, feed rate, depth of cut, and cutting radius) and the surface roughness criteria (*Ra* and *Rt*) for both ceramic cutting tools were obtained by multiple linear regressions. This correlation can be represented by the following equations:

CC650

$$Ra_{CC650} = 0.0151 + 0.544r - 4.017 \times 10^{-3} Vc + 11.1317f - 0.819ap - 6.683 \times 10^{-4} r \times Vc - 6.340r \times f - 0.396r \times ap + 0.010Vc \times f + 8.33 \times 10^{-3} Vc \times ap - 3.268f \times ap \quad (6)$$

$(R^2 = 91.33\ \%)$

$$Rt_{CC650} = +1.876 + 1.917r - 0.037Vc + 45.012f + 3.824ap + 5.699 \times 10^{-3} r \times Vc - 25.319r \times f - 6.918r \times ap + 0.105Vc \times f + 0.052Vc \times ap - 46.512f \times ap \quad (7)$$

$(R^2 = 86.24\ \%)$

CC6050

$$Ra_{CC6050} = -0.996 + 1.287r + 3.935 \times 10^{-3} Vc + 8.677f - 0.830ap - 7.447 \times 10^{-3} r \times Vc - 4.880r \times f + 0.301r \times ap + 0.019Vc \times f + 1.994 \times 10^{-3} Vc \times ap + 2.070f \times ap \quad (8)$$

$(R^2 = 96.82\ \%)$

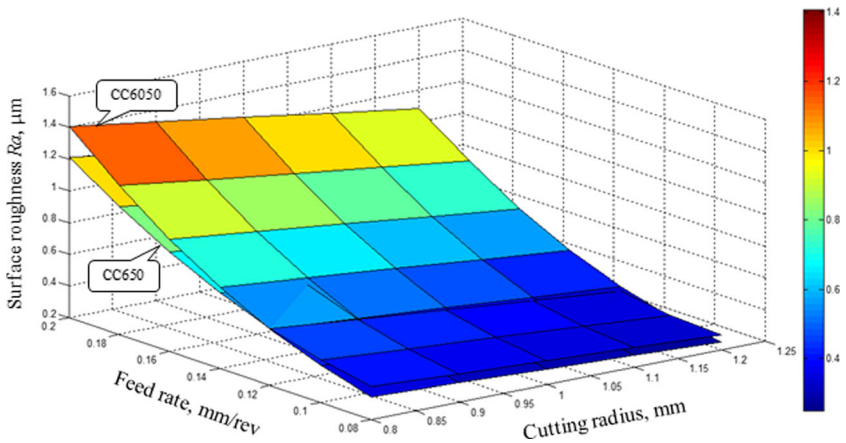

Fig. 3 3D surface plots for interaction effects of feed rate and cutting radius on arithmetic mean roughness *Ra* for (CC6050 and CC650)

$$Rt_{CC6050} = -0.240 + 2.1999r + 5.886 \times 10^{-3}Vc + 23.324f - 3.522ap - 0.022r \times Vc - 6.420r \times f + 1.614r \times ap + 0.093Vc \times f + 9.120 \times 10^{-3}Vc \times ap + 10.501f \times ap \quad (9)$$

($R^2 = 94.88\ \%$)

3.3 Surface topography

The two-factor interaction effects due to feed rate (f)–cutting radius (r), depth of cut (ap). and cutting speed (Vc) on surface roughness criteria (Ra and Rt) during hard turning of AISI H11 (50HRC) hot work tool steel were analyzed for two different ceramic inserts, namely coated ceramic tool CC6050 and uncoated ceramic tool CC650 through surface plots (Figs. 3, 4, 5, and 6). The 3D response surface plots were generated considering two machining parameters at a time, while the other parameters were kept at the middle levels.

From the interaction plot Figs. 3 and 4, it can be observed that, at constant cutting radius, the surface roughness criteria (Ra and Rt) increase with the increase of feed rates because their increase generate helicoid furrows, the result of tool shape and helicoids movement tool–workpiece. These furrows become deeper and broader when the feed rate increases [11]. For this reason, weak feed rate has to be employed during turning operation. Similar results were reported by Aouici et al. [2] when turning AISI D3 steel (60 HRC) using ceramic tool. On the other hand, surface roughness criteria have a tendency to decrease with an increase in cutting radius at constant feed rate. The best surface roughness was achieved at the lowest feed rate and highest cutting radius for both ceramic tools (CC6050 and CC650).

The analysis of response variable can be explained through surface plots too and a typical 3D surface plot is shown in Figs. 5 and 6. The surface plot illustrates that depth of cut and cutting speed increases at a constant feed rate and depth of cut, 0.14 mm/rev and 0.30 mm, respectively. As it can be deduced from these figures, the surface roughness criteria are not statistically significant. However, a qualitative comparison can be made. For example, Elbah et al. [16] found that the

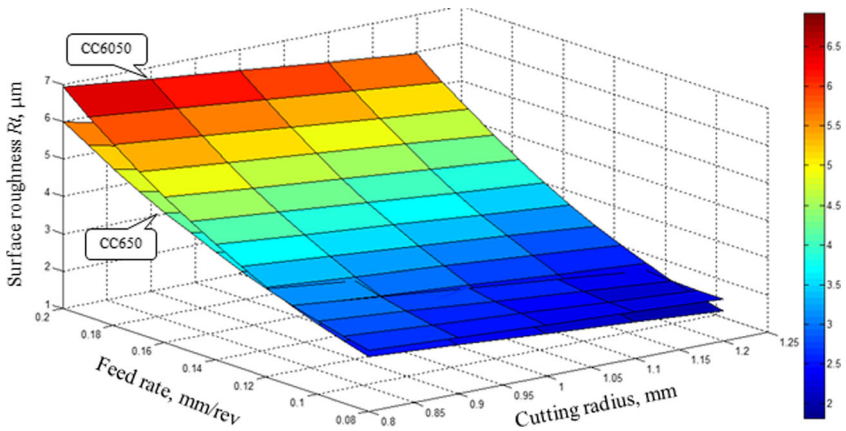

Fig. 4 3D surface plots for interaction effects of feed rate and cutting radius on total roughness for *Rt* (CC6050 and CC650)

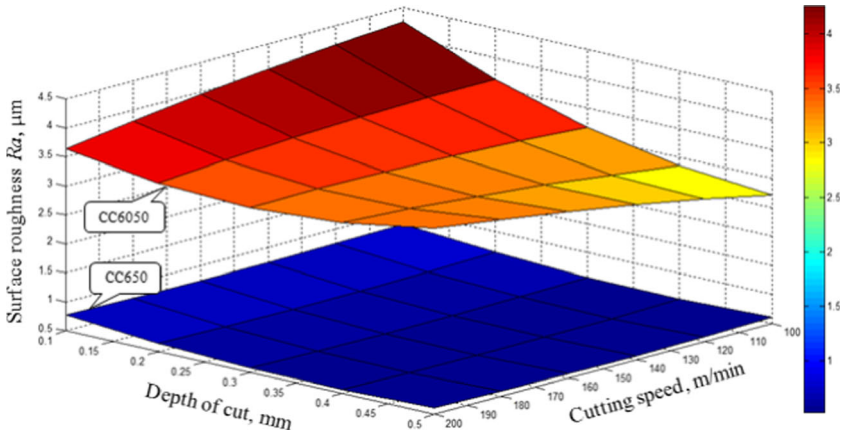

Fig. 5 3D surface plots for interaction effects of depth of cut and cutting speed on arithmetic mean roughness *Ra* for (CC6050 and CC650)

depth of cut does not impact on the surface roughness of turned surfaces. However, feed rate, nose radius, work material, and the tool point angle have a significant impact on the observed surface roughness using the fractional factorial experimentation approach [15]. In general, the CC650 tool gives lower value results than CC6050. In other term, uncoated ceramic cutting tool CC650 produces a better surface finish than the coated ceramic cutting tool CC6050.

3.4 2D and 3D surface topography

In this study, the surface integrity produced by turning of hardened hot work steel (AISI H11) with two different ceramic tools (CC6050 coated with TiN and uncoated mixed ceramic CC650) was characterized by means of 2D and 3D surface roughness.

The representative examples of 3D images of hard turned surfaces are visualized by four isometric views and contour maps. Characteristic sharp and partially blunt peaks localized by arrows are present in the scanned surfaces obtained for ceramics: CC6050 coated with TiN (Figs. 7a and 8a) and CC650 uncoated (Figs. 7b and 8b) tools at two noses radius (0.8 and 1.2) mm, respectively.

According to the graphs, it is noted that the both 3D profiles have represented pure roughness values, i.e., the turned surface topography in Figs. 7 and 8 shows well-defined peaks and valleys, this is mainly because when the turning operation process uses a single cutting edge, it generates helicoids furrows the result of tool shape and helicoids movement tool–workpiece. In addition, the two figures illustrate that a 1.2-mm cutting radius produces a highly precise surface (RaCC6050 = 0.162 µm and RaCC650 = 0.128 µm) compared to the other cutting radius with a 0.8-mm nose radius (RaCC6050 = 0.677 µm and RaCC650 = 0.643 µm). We also noticed from the 3D surface map that the insect with a noses radius of (1.2 mm) generates a small form of peaks and valleys this is because noses radius increases and this cause the increasing of the contact surface between the tool and the workpiece, which has the effect of crushing the asperities of the surface, and as a consequence roughness decreases. It has to be noticed that all surfaces were obtained by using new cutting edges, i.e., at the beginning of the tool life.

Figure 9 shows four exemplary of 2D surface profiles produced for the workpiece materials machined with two ceramics catting tools (CC6050 coated with TiN and CC650 uncoated, at two noses radius (0.8 and 1.2) mm). It must be noted that all the 2D profiles have represented pure roughness values, i.e., the waviness components have been filtered out.

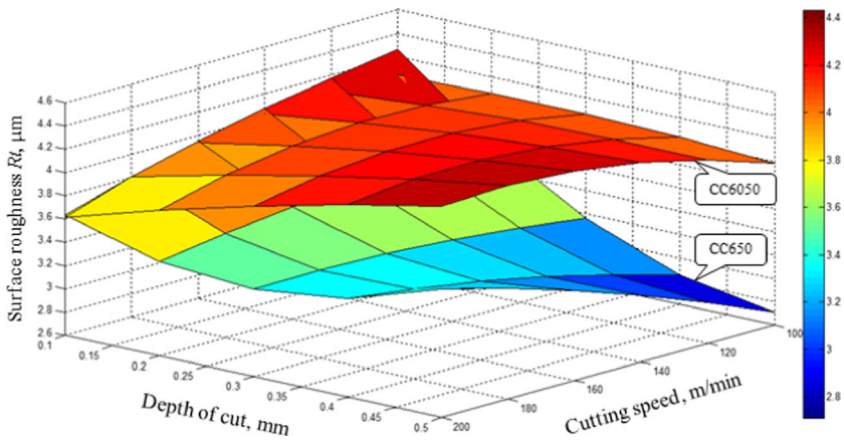

Fig. 6 3D surface plots for interaction effects of depth of cut and cutting speed on total roughness *Rt* for (CC6050 and CC650)

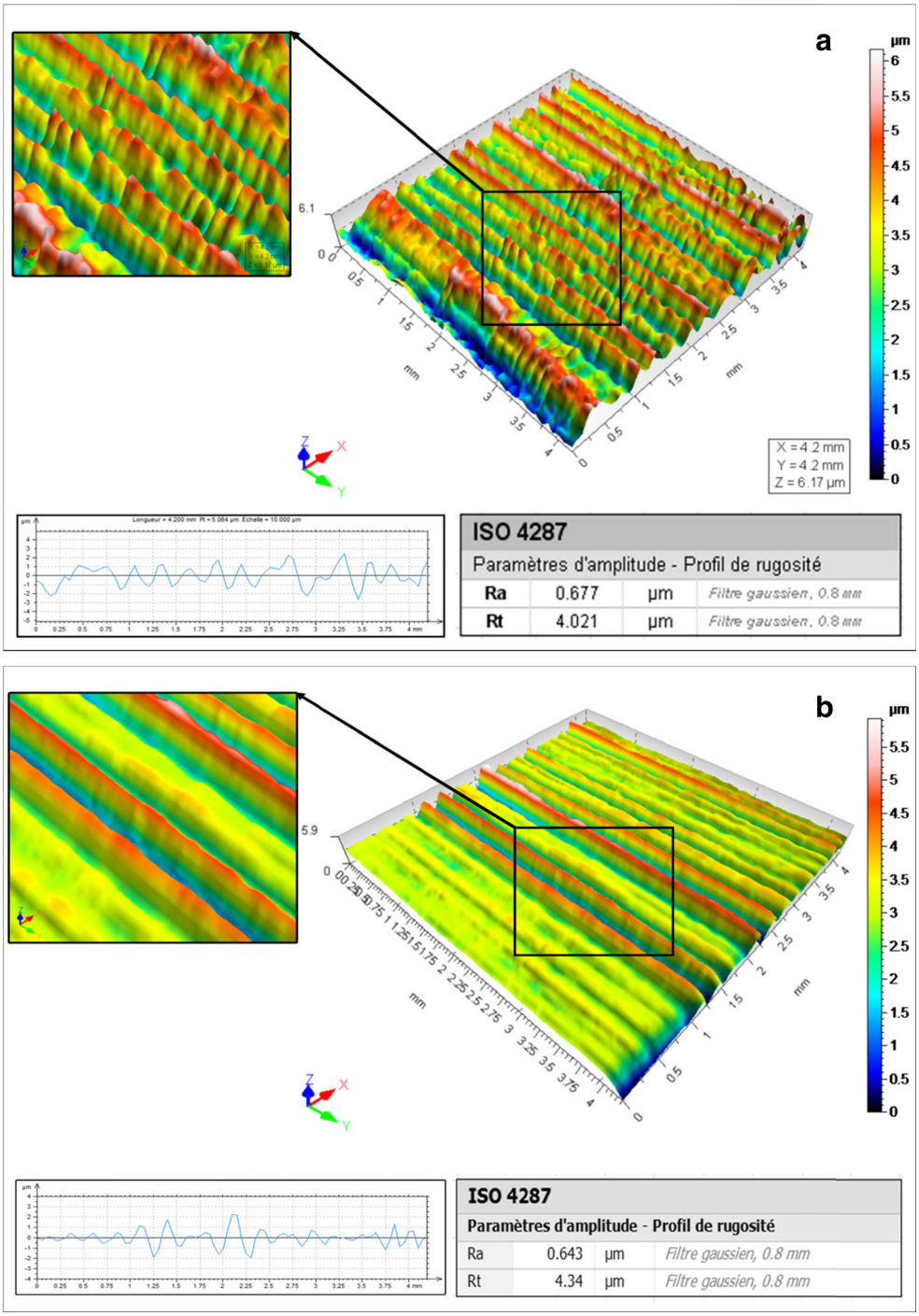

Fig. 7 3D topography for turning with **a** CC6050; **b** CC650 at $r = 0.8$ mm

The 2D profile along the feed direction for both ceramic cutting tools at high cutting radius (1.2 mm) shows a very small form of peaks and valleys compared to the profile with the small cutting radius (0.8 mm), this is because increasing cutting radius results the increase of the tool work contact length. It can be concluded that large tool nose radius gives only a finer surface finish. Earlier, Meddour et al. [24] observed that the use of small feed rate and large nose radius results the lowest surface roughness.

Figures 10 and 11 show the 3D surface topography, XY plane representation, and Abbott-Firestone Curve of the machined surfaces at two noses radius (0.8 and 1.2) mm using uncoated (CC650) and coated ceramic (CC6050) cutting tools. It can be noticed that the distribution of the peaks and valleys depends on the values of the noses radius. It is attributed to the helicoid furrow resulted from the combination of the tool–workpiece movement in turning using a single cutting edge. The surface roughness can be recognized by the

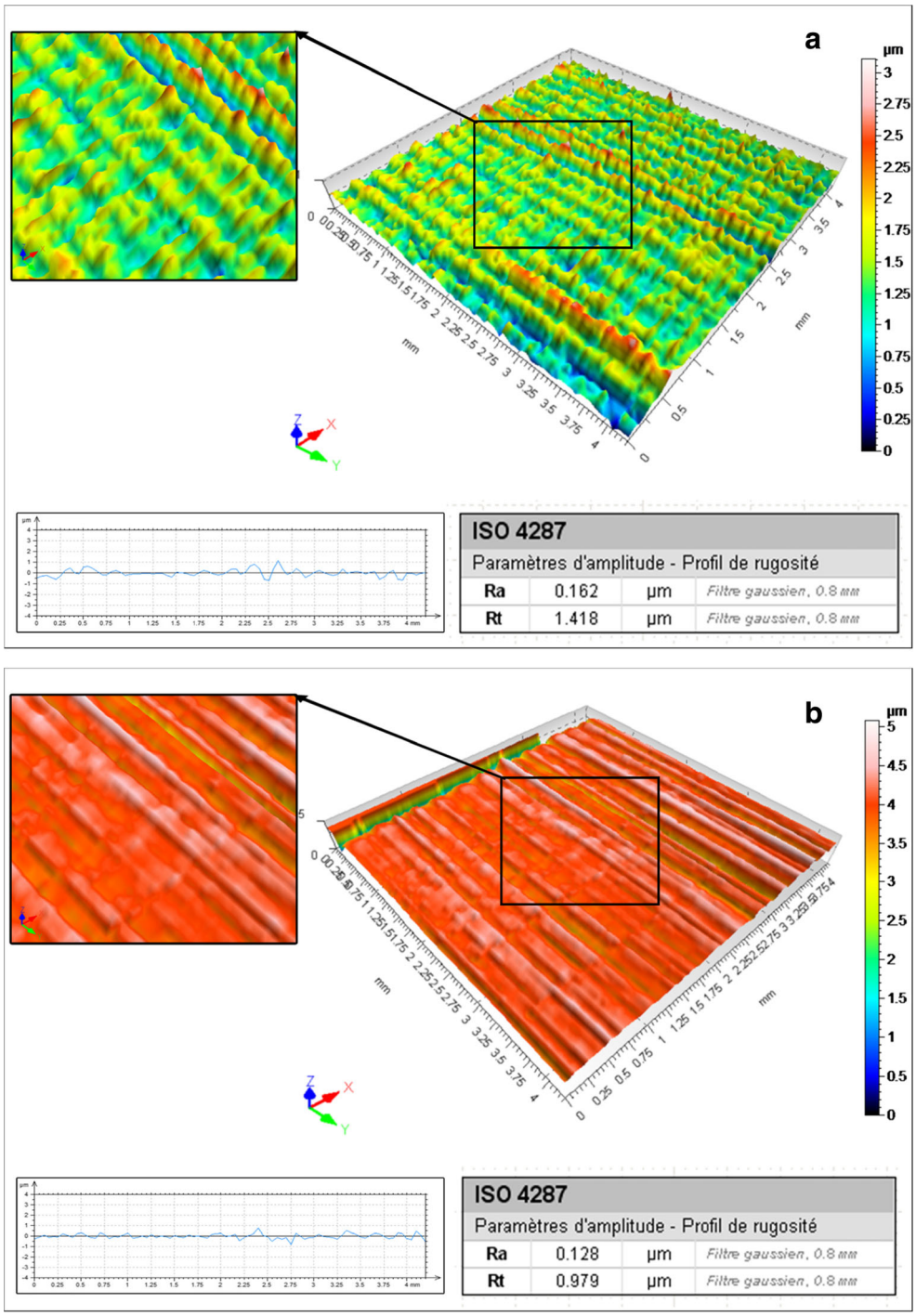

Fig. 8 3D topography for turning with **a** CC6050; **b** CC650 at $r = 1.2$ mm

variation in height of a surface, where a surface with less peak-to-valley height has a lower surface roughness. We also noticed from the 3D representation and XY plane representation of surface topography that the surfaces produced with a noses radius of 0.8 mm, having both the dark blue and red colors, can be representative of a larger variation in peak-to-valley height (Fig. 10(a1), Fig. 11(b1)), on the other hand the surfaces produced with a noses radius of 1.2 mm have almost unique colors which can be clearly illustrated in the surface generated with the uncoated insect with a noses radius of 1.2 mm (Fig. 10(a2)). From this figure, we can see that the entire surface are red, which mean it has a very small form of peaks and valleys, a proof that it is the best surface quality produced. Therefore, the uncoated ceramic insert (CC650) has the better performance compared with coated ceramic insert (CC6050) in terms of surface roughness of the workpiece. Similar results were found by Bensouilah et al. [5] when turning AISI D3 steel.

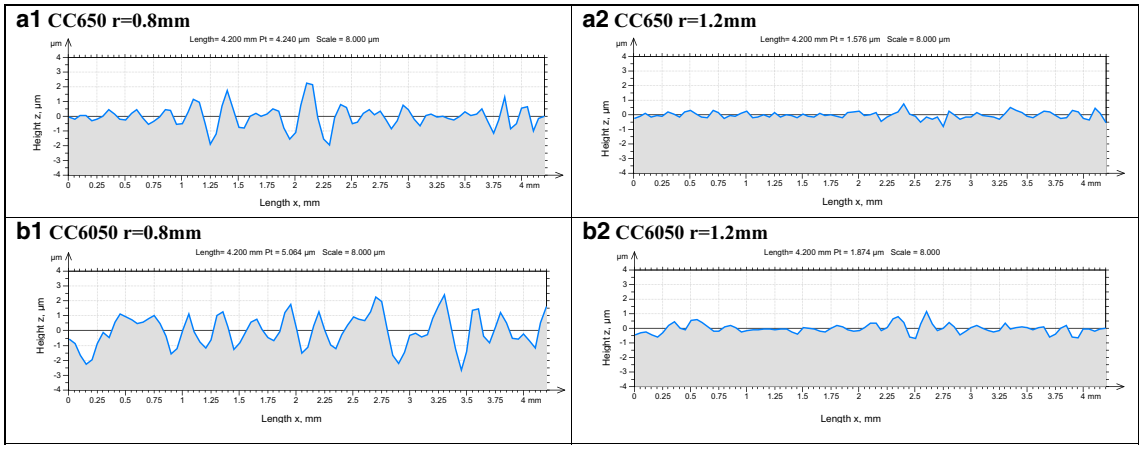

Fig. 9 2D surface profiles produced in dry hard turning with (CC650 and CC6050) at r = (0.8 and 1.2 mm)

Investigation of the depth histograms of the fourth surfaces obtained with the different inserts could provide additional information to compare their surface roughness. The solid red lines plotted on the histograms represent the bearing area curve (BAC), or Abbott-Firestone curve, calculated for the different inserts. The BAC is the integral of the amplitude distribution function and shows what percentage or linear fraction of a profile lies above a certain height. Dividing the BAC into subsections could help interpret the results of surface roughness. Abbott-Firestone curve is a good characteristic for assessing the functional properties of surfaces and their possible exploitation. We can distinguish between different surfaces with the same value of *Ra* or other height characteristics. Generally speaking, each type of surface is characterized by course of Abbott curve.

Dividing the BAC into subsections could help interpret the results of surface roughness. For this purpose, a straight line can be plotted based on a best-fit line over 40 % of the BAC's central portion. The three subsections of the BAC include core roughness depth (S_k), reduced peak height (S_{pk}), and reduced valley depth (S_{vk}). Figure 12e shows a schematic of the BAC curve and its three subsections. It is desirable to have a surface with a small S_{pk} because these peaks are worn off during the initial stages of service, while S_k can be the long-term characteristic (roughness) of a surface. According to Fig. 12, increasing the noses radius resulted in an upward translation of the BAC toward shallower depths. The figures illustrate that a 1.2-mm cutting radius produces a highly precise surface (S_{pk} CC6050 = 0.516 µm and S_{pk} CC650 = 0.373 µm) compared to the other cutting radius with a 0.8-mm nose radius (S_{pk}

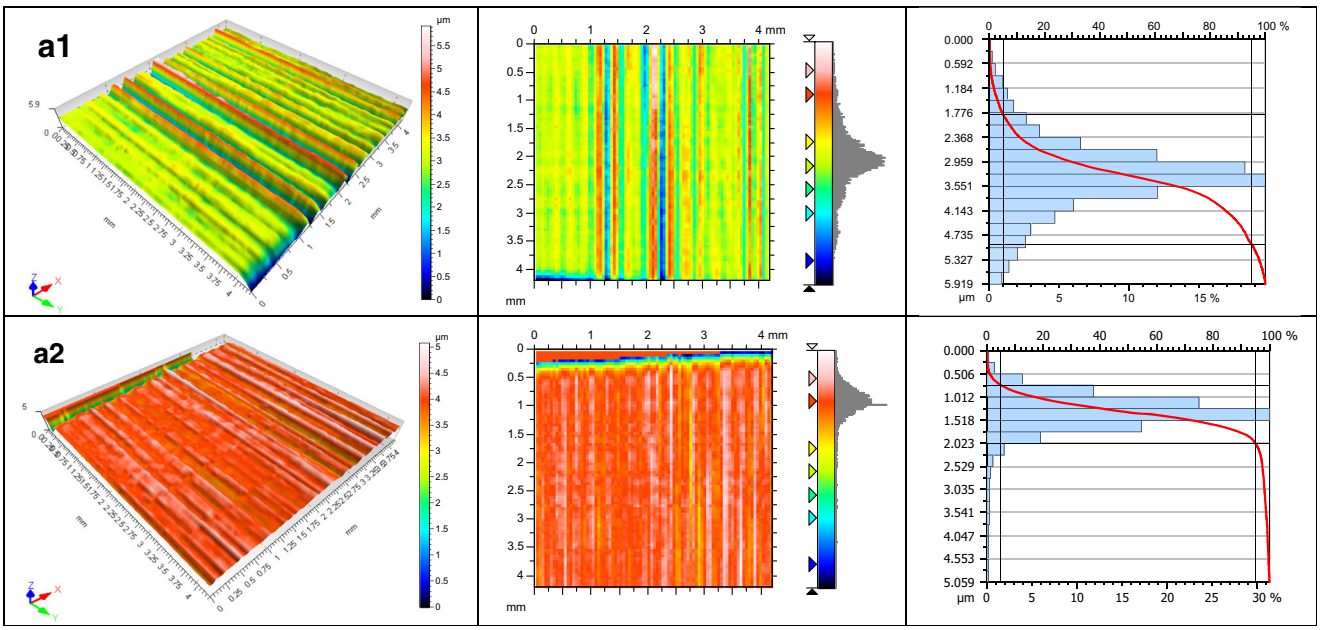

Fig. 10 3D representation, XY plane representation of surface topography, and Abbott-Firestone Curve for hard turning with CC650 insert: (*a1*) r = 0.8 mm, (*a2*) r = 1.2 mm

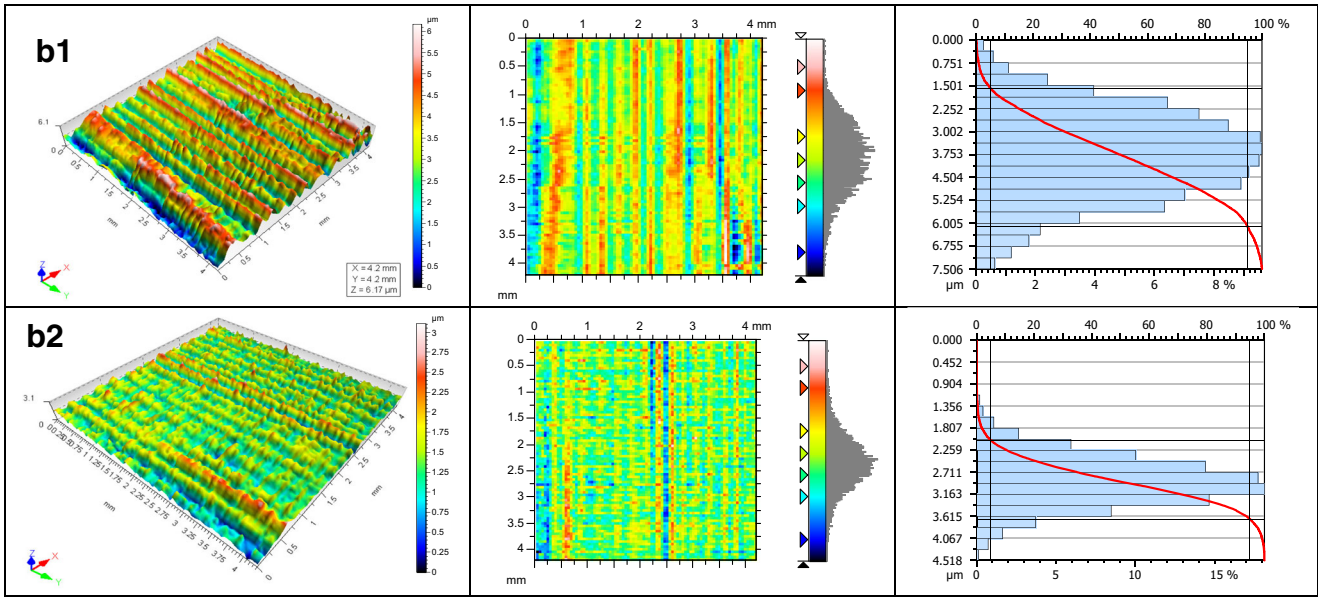

Fig. 11 3D representation, XY plane representation of surface topography, and Abbott-Firestone Curve for hard turning with CC6050 insert: (*b1*) $r = 0.8$ mm, (*b2*) $r = 1.2$ mm

CC6050 = 0.960 µm and S_{pk} CC650 = 1.23 µm). We also noticed from the Fig. 12b that the uncoated insect (CC650) with a noses radius of 1.2 mm had the minimum (S_k =0.809 µm) and (S_{pk} = 0.373 µm).

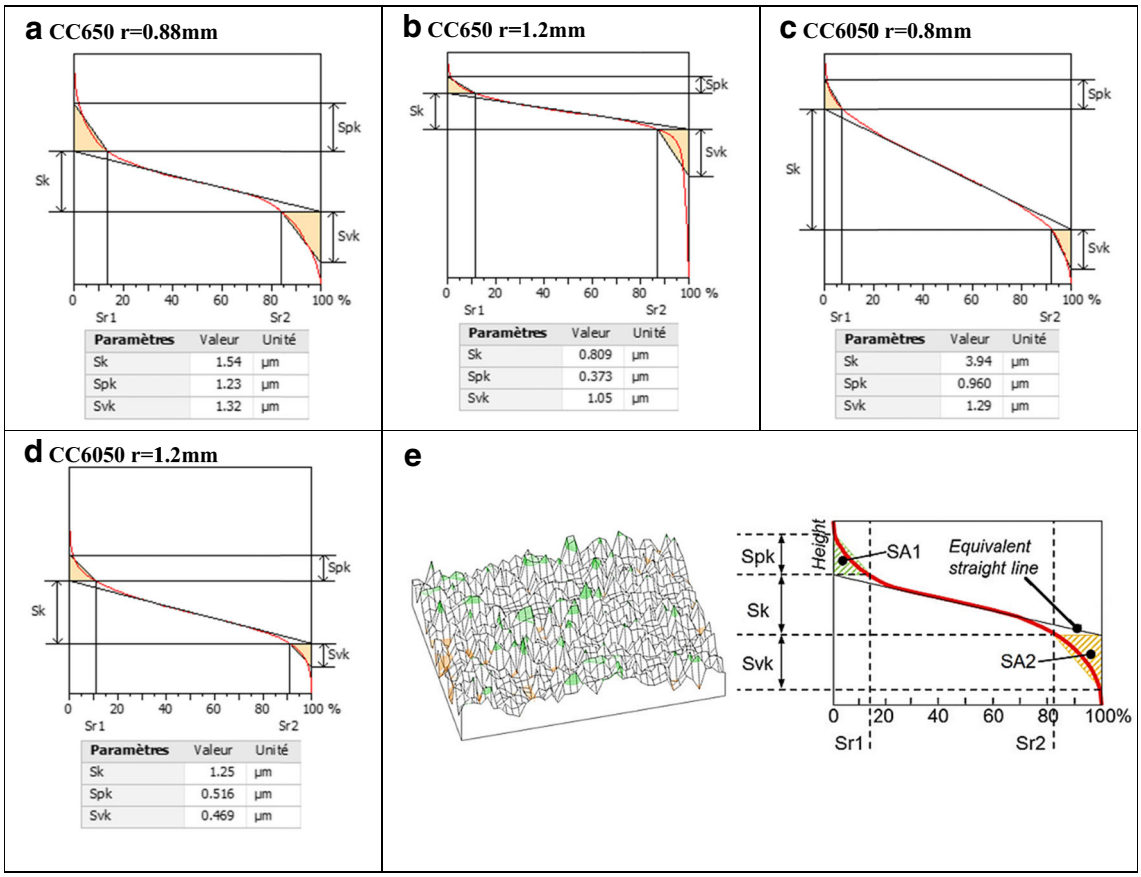

Fig. 12 The comparison of Abbot curves for the surfaces produced in dry hard turning with (CC650 and CC6050) at $r = (0.8$ and 1.2 mm); **e** schematic illustration of the BAC

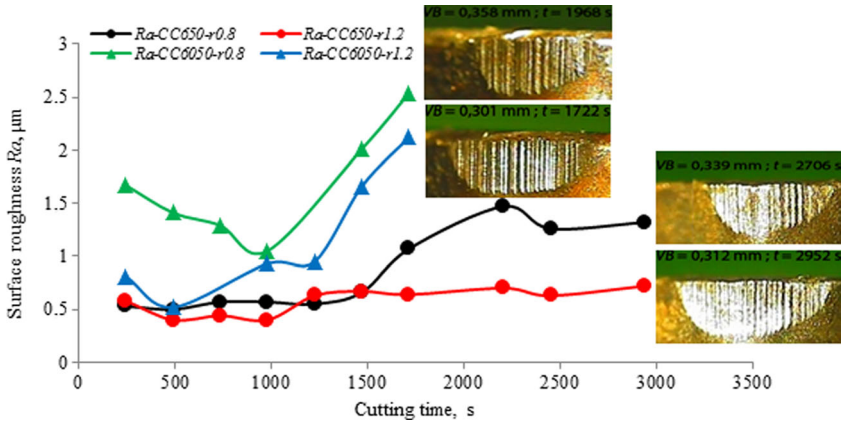

Fig. 13 Influence of time on arithmetic mean roughness *Ra*, at various cutting radius for $Vc = 150$ m/min, $f = 0.08$ mm, and $ap = 0.30$ mm (CC6050 and CC650)

3.5 Surface roughness evolution

Surface roughness is one of the most important requirements in machining process. The surface roughness value is a result of the tool wear. When tool wear increase, the surface roughness also increases. The determination of the sufficient cutting parameters is a very important process obtained by means of both minimum surface roughness values and long tool life. In this section, the roughness of the machined surface was also measured as a function of cutting time, and hence as a function of tool wear. The effect of the cutting time on the machined surface is often discussed in hard machining studies. Pavel et al. [26] showed such dependence for two types of CBN inserts while the *Ra* was within 1.18–1.48 µm for 38 min. Grzesik and Wanat [20] obtained *Ra* dependence for commercial CC650 ceramics within 0.55–0.85 µm for 28 min of cutting. De Oliveira et al. [12] reported that $Ra = 0.55$–0.60 µm as a linear dependence of time $tc = 20$ min.

A series of experiments were carried out in order to determine the effect of cutting time (hence flank wear) on machined surface roughness using the same cutting conditions: $Vc = 150$ m/min; $f = 0.08$ mm/rev, and $ap = 0.30$ mm. Surface roughness measurements were taken at every 100 mm length cut. Three readings were taken at three different points on the circumference, which was 120° apart. The averages of these readings are plotted on the graphs. Figures 13 and 14 illustrate these effects for the CC6050 and CC650, respectively. The analysis shows that the surface roughness criteria produced using a coated ceramic insert CC6050 is superior to the surface produced using an insert with uncoated insert at various cutting radius. Also, it can be seen from Figs. 13 and 14 that the relationship may be explained as follows.

The first zone when the cutting time is inferior to 16 min, the inserts CC650 and CC6050 provide a better surface finish at all cutting radius. Example, for a time $t = 10$ min, it recorded wears $VB_{CC6050} = 0.189$ mm, $VB_{CC650} = 0.209$ mm, which correspond to the surface roughness criteria ($Ra_{1.2}$ and $Rt_{1.2}$) with the values of (0.93 and 6.90) µm for CC6050 and the values (0.40 and 2.88) µm for CC650 insert.

When the development of excessive flank wear is superior to 16 min, increased cutting force and temperature may destabilize the machining process and the surface quality is degraded. For example, at the end of machining, it has been recorded that tool life $T_{CC6050} = 28$ min, $T_{CC650} = 49$ min, which corresponds to the surface

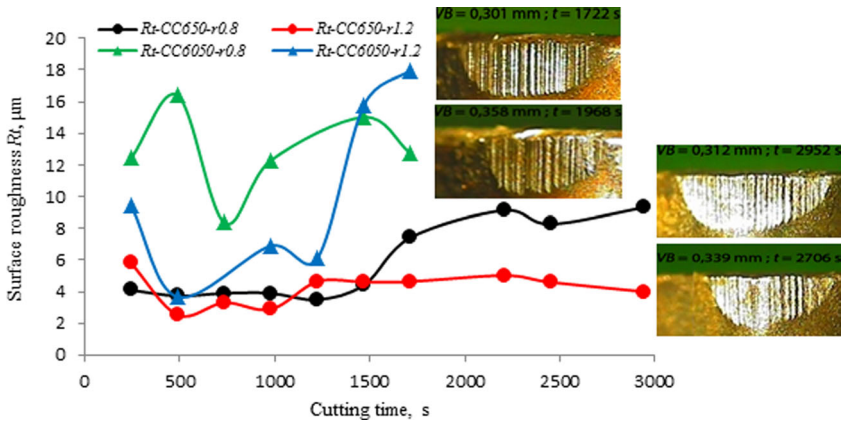

Fig. 14 Influence of time on total roughness *Rt*, at various cutting radius for $Vc = 150$ m/min, $f = 0.08$ mm, and $ap = 0.30$ mm (CC6050 and CC650)

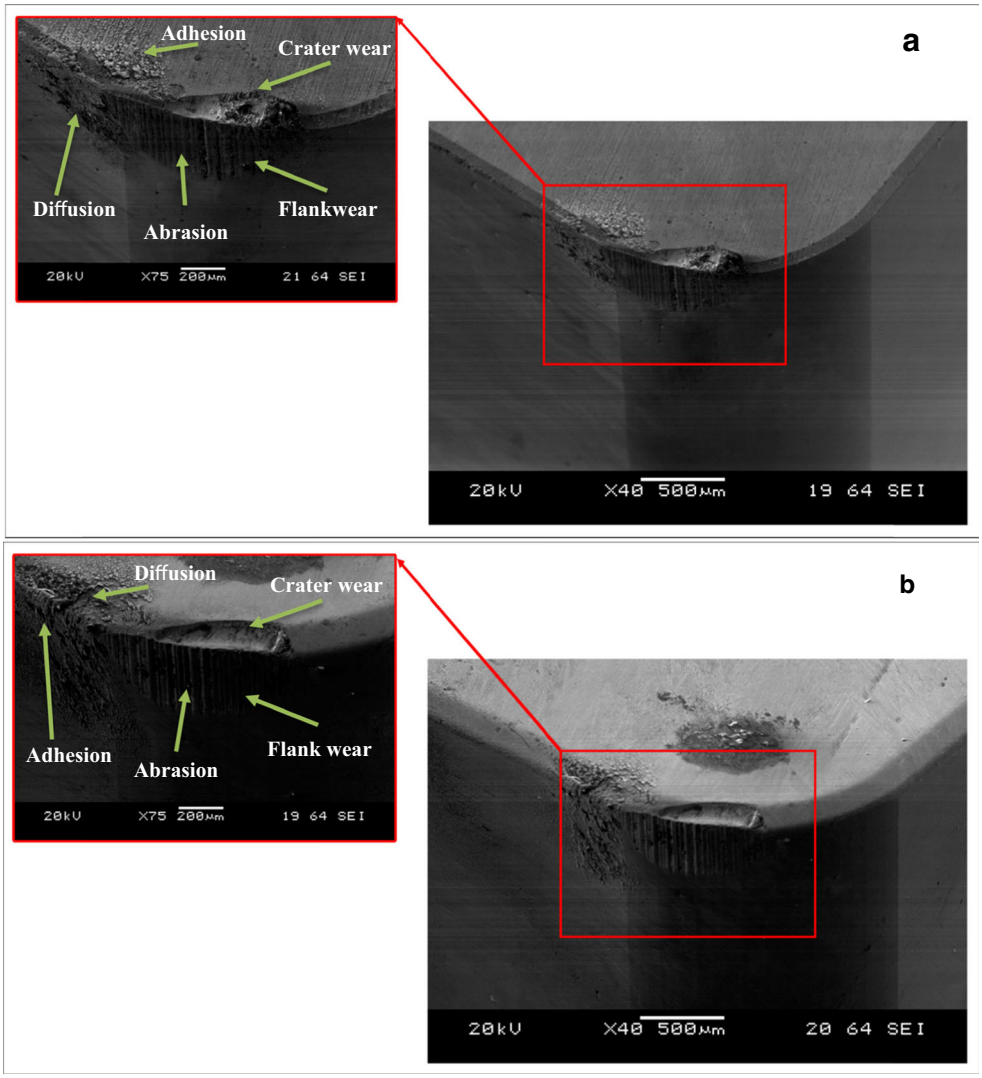

Fig. 15 SEM images of the flank and crater wears of a cutting tools: **a** CC6050; **b** CC650 at $Vc = 150$ m/min, $f = 0.08$ mm/rev and $ap = 0.30$ mm for $r = 1.2$ min

roughness criteria ($Ra_{1,2}$ and $Rt_{1,2}$) with the values of (2.12 and 18) µm for CC6050 insert and the values of (0.72 and 4.64) µm for CC650 insert.

The Fig. 15 represents the scanning electron micrographs for the rake and clearance faces of the ceramics cutting tools (CC6050 and CC650) after turning of AISI H11 (50 HRC) at cutting radius of 1.2 mm, with cutting speed, feed rate, and depth of cut values of 150 m/min, 0.08 mm/rev, and 0.30 mm, respectively. This figure shows the typical aspect under an optical microscope of the flank wear face of ceramic tools

Table 6 Constraints for optimization of cutting conditions

Condition	Goal	Lower limit		Upper limit		Lower weight	Upper weight	Importance
		CC650	CC6050	CC650	CC6050	1	1	3
Cutting radius (mm)	Is in range	0.80		1.20		1	1	3
Cutting speed (Vc)	Is in range	100		200		1	1	3
Feed rate (f)	Is in range	0.08		0.20		1	1	3
Depth of cut (ap)	Is in range	0.10		0.50		1	1	3
Ra (µm)	Minimize	0.2	0.18	1.36	1.51	1	1	3
Rt (µm)	Minimize	0.69	1.33	6.77	7.96	1	1	3

Table 7 Response optimization for surface roughness parameters (CC650 and CC6050)

Test no.	Machining parameters				Surface roughness		Desirability	Remarks
	r	*Vc*	*f*	*ap*	*Ra*	*Rt*		
Solutions CC650								
1	1.031	199.999	0.08	0.1	0.2	1.126	0.963	Selected
2	1.024	200	0.08	0.1	0.201	1.124	0.963	
3	1.049	199.998	0.08	0.1	0.197	1.133	0.963	
4	1.006	200	0.08	0.1	0.203	1.118	0.963	
5	1.067	200	0.08	0.1	0.195	1.138	0.962	
Solutions CC6050								
1	1.198	183.712	0.081	0.101	0.149	1.283	1	Selected
2	1.124	197.728	0.081	0.101	0.147	1.315	1	
3	1.155	190.534	0.08	0.108	0.146	1.297	1	
4	1.164	195.123	0.082	0.131	0.145	1.318	1	
5	1.191	188.759	0.081	0.162	0.143	1.311	1	

after testing. The micrographs were taken at the end of tool life (total machining time is shown in brackets). The analysis of the micrographs shows that abrasion, diffusion, and adhesion are prominent wear mechanisms, especially for the flank and clearance faces. However, along with the nose wear, crater wear also can be seen for all the tools, indicating diffusion wear, especially for the rake face as one of the active wear mechanisms along with the abrasion and adhesion wear mechanisms. In conclusion, the abrasive wear has been frequently reported as a main wear mechanism in hard turning. Due to the high temperature and high stresses in hard turning, diffusion wear may also occur. Chemical reactions, including oxidation at high speeds due to high cutting temperatures, have also been reported. Chemical properties may be very important at the high cutting speeds in which the cutting temperature could accelerate any chemical reaction between the tool and workpiece.

4 Optimization of responses

In the present study, the desirability function approach of the RSM has been employed for surface roughness optimization. The optimization module searches for a combination of factor levels that simultaneously satisfy the requirements placed on each of the responses and factors in an attempt to establish the appropriate model. During the optimization process, the aim is to find the optimal values of machining parameters in order to produce the lowest surface roughness (*Ra* and *Rt*). To resolve this type of parameter design problem, an objective function, $F(x)$, is

$$DF = \left(\prod_{i=1}^{n} d_i^{wi} \right)^{\frac{1}{\sum_{j-1}^{n} wi}} \qquad (10)$$

$$F(x) = -DF$$

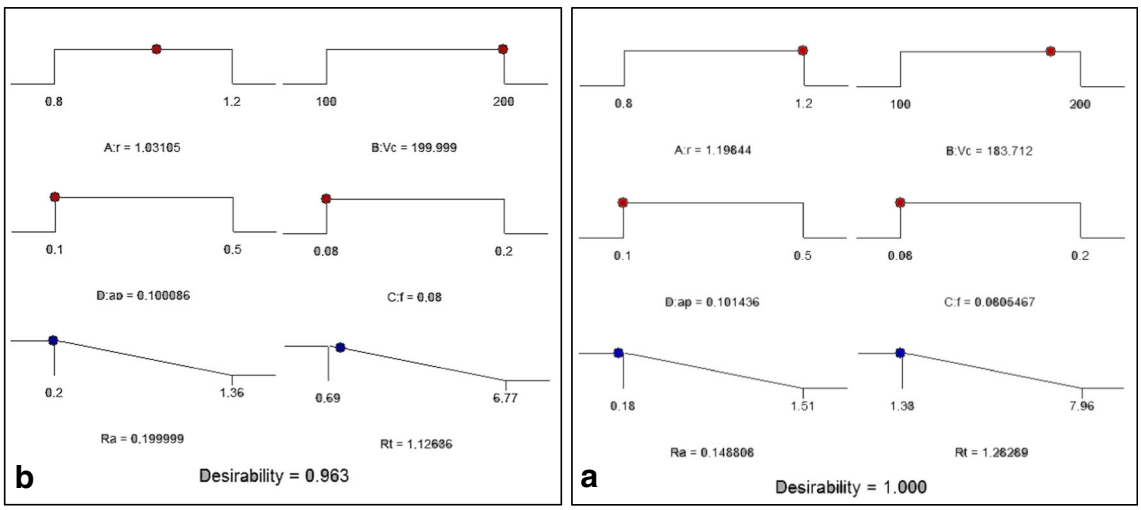

Fig. 16 Ramp function graph for surface roughness (*Ra* and *Rt*) with **a** CC6050 and **b** CC650 inserts

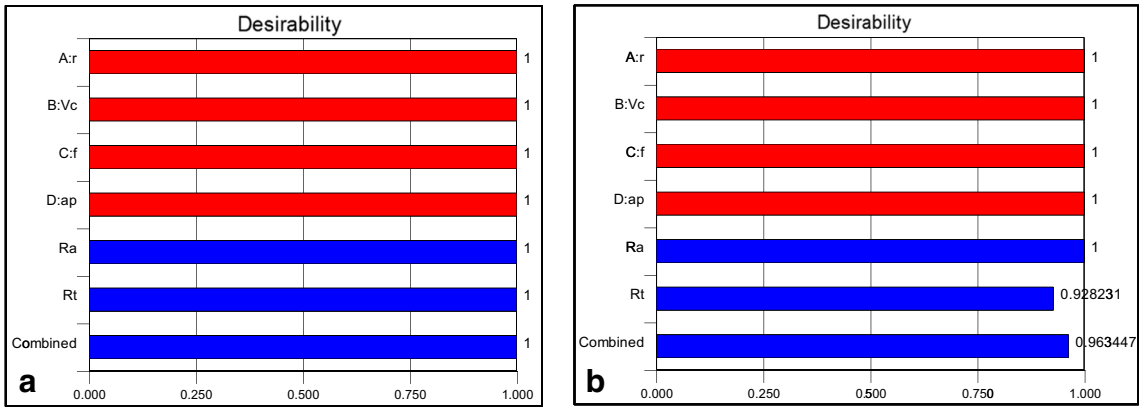

Fig. 17 Bar graph of desirability with **a** CC6050 and **b** CC650 inserts

Where d_i is the desirability defined for the ith targeted output and w_i is the weighting of d_i.

For various goals of each targeted output, the desirability d_i can be defined in different forms. If the goal is to reach a specific value of T_i, the desirability d_i is written as:

$$\begin{aligned} d_i &= 0 \quad \text{if} \quad Y_i \le Low_i \\ d_i &= \left[\frac{Y_i - Low_i}{T_i - Low_i}\right] \quad \text{if} \quad Low_i \le Y_i \le T_i \\ d_i &= \left[\frac{Y_i - High_i}{T_i - High_i}\right] \quad \text{if} \quad T_i \le Y_i \le High_i \\ d_i &= 0 \quad \text{if} \quad Y_i \ge High_i \end{aligned} \tag{11}$$

In the case of searching for a maximum, the desirability is rewritten as follows:

$$\begin{aligned} d_i &= 0 \quad \text{if} \quad Y_i \le Low_i \\ d_i &= \left[\frac{Y_i - Low_i}{High_i - Low_i}\right] \quad \text{if} \quad Low_i \le Y_i \le High_i \\ d_i &= 1 \quad \text{if} \quad Y_i \ge High_i \end{aligned}$$

In the case of searching for a minimum, the desirability can be defined by the following equations:

$$\begin{aligned} d_i &= 1 \quad \text{if} \quad Y_i \ge Low_i \\ d_i &= \left[\frac{High_i - Y_i}{High_i - Low_i}\right] \quad \text{if} \quad Low_i \le Y_i \le High_i \\ d_i &= 0 \quad \text{if} \quad Y_i \ge High_i \end{aligned} \tag{12}$$

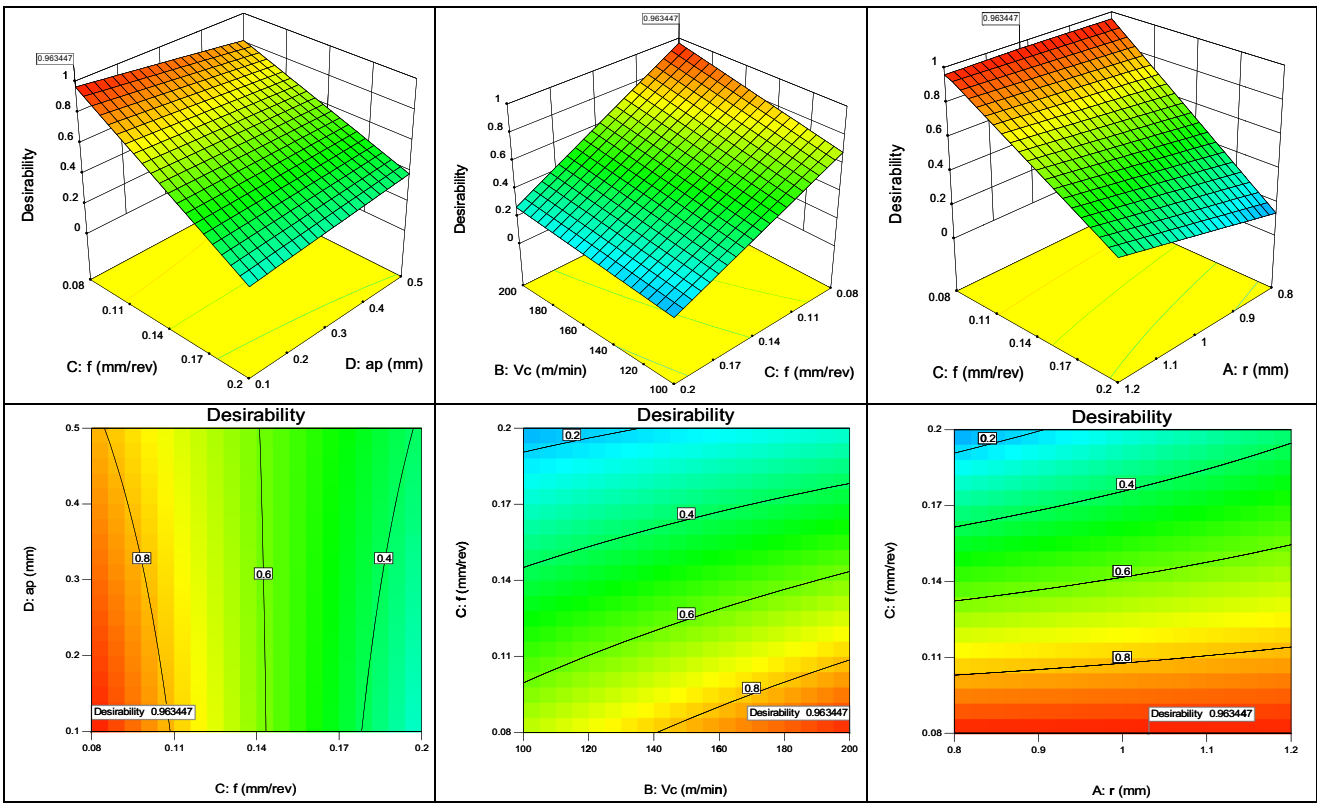

Fig. 18 3D surface plot and contour graph of optimization combined for CC650 insert

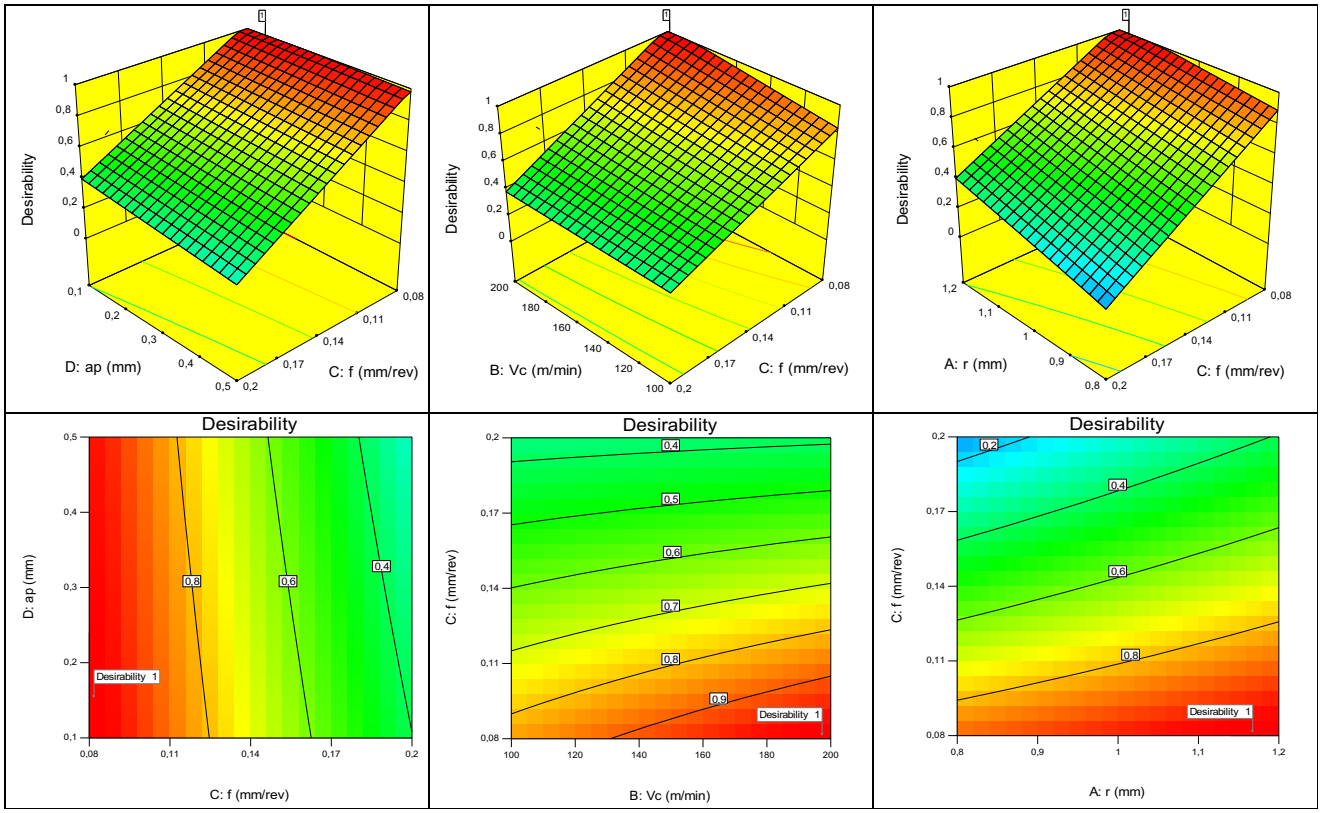

Fig. 19 3D surface plot and contour graph of optimization combined for CC6050 inserts

Where the Y_i is the found value of the ith output during optimization processes, the Low_i and the $High_i$ are, respectively, the minimum and the maximum values of the experimental data for the ith output. In Eq. 12, w_i is set to 1 since the d_i is equally important in this study. The DF is a combined desirability function, and the objective is to choose an optimal setting that maximizes a combined desirability function DF, i.e., minimizes $F(x)$.

The constraints used during the optimization process are summarized in Table 6. The optimal solutions are reported in Table 7 for both ceramic cutting tools CC650 and CC6050 in order to decrease the desirability level. The optimum cutting parameters obtained with the importance degrees of 3 for *Ra* and *Rt* are chosen in terms of the highest desirability value (Figs. 18 and 19). The desirability levels are decreased when the operating parameter is changing. So, we can conclude that in the highest cutting radius, highest cutting speed, and lowest feed rate with lowest depth of cut, the performances of the cutting tool are optimized and the desirability levels are (100 and 96.30) % in these optimized conditions for both ceramic cutting tools CC650 and CC6050, respectively.

The Fig. 16 and Table 7 show the optimization results. Values of optimal cutting parameters are found to be with cutting speed of (199.999 and 183.712) m/min, feed rate of (0.08 and 0.081) mm/rev, cutting depth of (0.1 and 0.101) mm, and cutting radius of (1.031 and 1.198) mm. The predicted

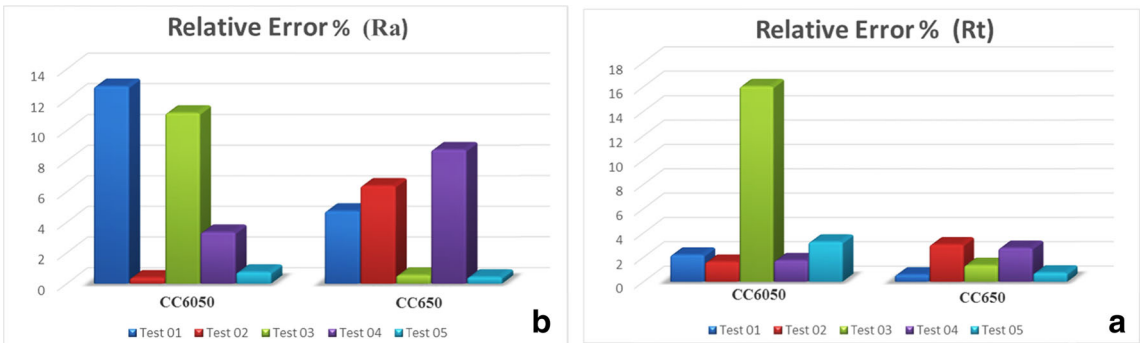

Fig. 20 Relative errors between experimental and predicted values: **a** *Ra* and **b** *Rt* for both ceramic cutting tools (CC650 and CC6050)

Table 8 Confirmation experiments

Exp. no.	Designing parameters				For regression equations					
	Vc (m/min)	*f* (mm/rev)	*ap* (mm)	*r* (mm)	Exp.	Pred.	Error %	Exp.	Pred.	Error %
					CC6050			CC650		
Surface roughness (*Ra*)										
1	129	0.09	0.15	0.8	0.47	0.4095	12.8723	0.45	0.4713	4.7333
2	153	0.11	0.25	0.8	0.57	0.5722	0.3860	0.57	0.5336	6.3860
3	195	0.18	0.4	0.8	1.44	1.2795	11.1458	0.97	0.9646	0.5567
4	129	0.09	0.15	1.2	0.37	0.3824	3.3514	0.37	0.4024	8.7568
5	153	0.11	0.25	1.2	0.45	0.4466	0.7556	0.39	0.3917	0.4359
Surface roughness (*Rt*)										
1	129	0.09	0.15	0.8	2.77	2.7091	2.1986	2.81	2.7936	0.5836
2	153	0.11	0.25	0.8	3.32	3.3735	1.6114	3.32	3.2189	3.0452
3	195	0.18	0.4	0.8	7.56	6.3489	16.0198	5.32	5.2483	1.3477
4	129	0.09	0.15	1.2	2.28	2.3196	1.7368	2.46	2.5279	2.7602
5	153	0.11	0.25	1.2	2.88	2.7859	3.2674	2.51	2.5286	0.7410

responses are $Ra = (0.2$ and $0.149)\,\mu m$, and (1.126 and 1.283) μm for *Rt*, with desirability value of (0.963 and 1) for both ceramic cutting tools CC650 and CC6050, respectively.

Figure 17 presents the bar graph of desirability for the cutting conditions and the responses together with a combined desirability = (0.963 and 1) for (CC650 and CC6050) (Figs. 18 and 19).

5 Confirmation experiments

In order to verify the adequacy of the model developed, five new trials were performed for both ceramic cutting tools (CC650 and CC6050); the test conditions for the confirmation test were chosen so that they are within the range of the levels defined previously. The predicted values and the associated experimental values are compared (Fig. 20). The error percentage is within permissible limits (Table 8). The data from the confirmation runs and their comparisons with the predicted design for surface roughness (*Ra*) and (*Rt*) are listed in Table 8. Based on the analysis of Table 8 results, it can be observed that the calculated error is small. The relative errors between experimental and predicted values for (*Ra*) and (*Rt*) for both ceramic cutting tools (CC650 and CC6050) are obtained in the range of [(0.4359 to 8.7568 %) and (0.5836 to 3.0452)] and [(0.3860 to 12.8723 %) and (1.6114 to 16.0198 %)], respectively. All the experimental values for the confirmation run are within the 95 % prediction interval. Obviously, the quadratic model obtained is excellently accurate.

6 Conclusion

Based on the above results for the hard turning of AISI H11 steel with 50 HRC using both cutting tools namely, coated CC6050 and uncoated CC650 ceramic tools under conditions similar to those used in this work, the following conclusions are made:

1. This study shows that the surface roughness *Ra* is strongly influenced by the feed rate. Its contribution is (72.245 and 89.953) %, for CC650 and CC6050 tools, respectively. Additionally, this study confirms that in dry straight turning of this steel (AISI H11) and for the cutting conditions tested, the uncoated ceramic is better than coated ceramic in terms of surface roughness and wear resistance. The ratio mean value for Ra_{CC650}/Ra_{CC6050} and Rt_{CC650}/Rt_{CC6050} is of (0.89 and 0.85), respectively.
2. The linear mathematical models developed for surface roughness using regression analysis technique are very useful for predicting new experiments. Close correlation between predicted and measured values was established.
3. The 3D visualization map of the machined surface is an important investigation tool. It confirmed some characteristic features of surfaces produced with both inserts tested, i.e., peaks and valleys.
4. Based on the response surface optimization and the composite desirability method of RSM, the optimal turning parameters of AISI H11 steel with two ceramic cutting tools CC650 and CC6050, respectively, are found to be $Vc = (199.999$ and $183.712)$ m/min, $f = (0.08$ and $0.081)$ mm/rev, $ap = (0.1$ and $0.101)$ mm, and $r = (1.031$ and $1.198)$ mm. The optimized responses are $Ra = (0.2$

and 0.149) μm, and (1.126 and 1.283) μm for *Rt*, with desirability value of (0.963 and 1).

5. Flank wear is an important factor to consider. Its evolution damages the surface finish of the workpiece. Even so when [*VB*] is 0.3 mm, the average roughness *Ra* did not exceed 2.12 μm for CC6050.
6. From the confirmation test, it can be said that the empirical models developed are reasonably accurate. The relative errors between experimental and predicted values for (*Ra*) and (*Rt*) for both ceramic cutting tools (CC650 and CC6050) are obtained in the range of [(0.4359 to 8.7568 %) and (0.5836 to 3.0452)] and [(0.3860 to 12.8723 %) and (1.6114 to 16.0198 %)], respectively.

References

1. Aouici H, Yallese MA, Elbah M, Fnides B, Chaoui K, Mabrouki T (2011) Modeling and optimization of hard turning of X38CrMoV5-1 steel with CBN tool: machining parameters effects on flank wear and surface roughness. J Mech Sci Technol 25(11):2843–2851
2. Aouici H, Bouchelaghem H, Yallese MA, Elbah M, Fnides B (2014) Machinability investigation in hard turning of AISI D3 cold work steel with ceramic tool using response surface methodology. J Adv Manuf Technol 73:1775–1788
3. Bartarya G, Choudhury SK (2012) State of the art in hard turning. Int J Mach Tools Manuf 53:1–14
4. Benga GC, Abrão AM (2003) Turning of hardened 100Cr6 bearing steel with ceramic and PCBN cutting tools. J Mater Process Technol 143–144:237–241
5. Bensouilah H, Aouici H, Meddour I, Yallese MA, Mabrouki T, Girardin F (2016) Performance of coated and uncoated mixed ceramic tools in hard turning process. Measurement 82:1–18
6. Boothroyd G, Knight WA (1989) Fundamentals of machining and machine tools. Marcel Dekker, New York
7. Bouacha K, Yallese MA, Mabrouki T, Rigal J-F (2010) Statistical analysis of surface roughness and cutting forces using response surface methodology in hard turning of AISI 52100 bearing steel with CBN tool. Int J Refract Metals Hard Mater 28:349–361
8. Bouzid L, Yallese MA, Chaoui K, Mabrouki T, Boulanouar L (2014) Mathematical modeling for turning on AISI 420 stainless steel using surface response methodology. Proc. IMechE Part B: J. Eng. Manuf. 1–17.
9. Darwish SM (2000) The impact of the tool material and the cutting parameters on surface roughness of supermet 718 nickel superalloy. J Mater Process Technol 97:10–18
10. Davim JP (2010) Machining of hard materials. Springer, London. doi: 10.1007/978-1-84996-450-460.
11. de Godoy VAA, Diniz AE (2011) Turning of interrupted and continuous hardened steel surfaces using ceramic and CBN cutting tools. J Mater Process Technol 211:1014–1025
12. De Oliveira AJ, Diniz AE, Ursolino DJ (2009) Hard turning in continuous and interrupted cut with PCBN and whisker-reinforced cutting tools. J Mater Process Technol 209:5262–5270
13. Dilbag SP, Venkateswara RA (2007) Surface roughness prediction model for hard turning process. J Adv Manuf Technol 32:1115–1124
14. Dureja JS, Gupat VK, Sharma VS, Dogra M (2009) Design optimization of cutting conditions and analysis of their effect on tool wear and surface roughness during hard turning of AISI-H11 steel with a coated-mixed ceramic tool. J Eng Mnuf 223:1441–1450
15. El Baradie MA (1991) Computer aided analysis of a surface roughness model for turning. J Mater Process Technolo 26:207–216
16. Elbah M, Yallese MA, Aouici H, Mabrouki T, Rigal J (2013) Comparative assessment of wiper and conventional ceramic tools on surface roughness in hard turning AISI 4140 steel. Measurement 46:3041–3056
17. Fnides B, Aouici H, Yallese MA (2008) Cutting forces and surface roughness in hard turning of hot work steel X38CrMoV5-1 using mixed ceramic. MECHANIKA 2(70):73–78
18. Fnides B, Boutabba S, Fnides M, Aouici H, Yallese MA (2013) Cutting tools flank wear and productivity investigation in straight turning of X38CrMoV5-1 (50 HRC). J App Eng Technol 3(1):1–10
19. Grzesik W (2009) Wear development on wiper Al2O3–TiC mixed ceramic tools in hard machining of high strength steel. Wear 266: 1021–1028
20. Grzesik W, Wanat T (2005) Comparative assessment of surface roughness produced by hard machining with mixed ceramic tools including 2D and 3D analysis. J Mater Process Technol 169:364–371
21. Huang Y, Dawson TG (2005) Tool crater wear depth modeling in CBN hard turning. Wear 258(9):1455–1461
22. Jenn-Tsong H, Nun-Ming L, Ko-Ta C (2008) Investigating the machinability evaluation of Hadfield steel in the hard turning with Al_2O_3/TiC mixed ceramic tool based on the response surface methodology. J Mater Process Technol 208:532–541
23. Lima JG, Ávila RF, Abraõ AM, Faustino M, Davim JP (2005) Hard turning: AISI 4340 high strength low alloy steel and AISI D2 cold work tool steel. J Mater Process Technol 169:388–395
24. Meddour I, Yallese MA, Khattabi R, Elbah M, Boulanouar L (2015) Investigation and modeling of cutting forces and surface roughness when hard turning of AISI 52100 steel with mixed ceramic tool: cutting condition optimization. Int J Adv Manuf Technol. doi: 10.1007/s00170-014-6559-z.
25. Paiva AP, Campos PH, Ferreira JR, Lopes LGD, Paiva EJ, Balestrassi PP (2012) A multivariate robust parameter design approach for optimization of AISI 52100 hardened steel turning with wiper mixed ceramic tool. Int J Refract Metals Hard Mater 30:152–163
26. Pavel R, Marinescu I, Deis M, Pillar J (2005) Effect of tool wear on surface finish for a case of continuous and interrupted hard turning. J Mater Process Technol 170:341–349
27. Poulachon G, Bandyopadhyay BP, Jawahir IS, Pheulpin S, Seguin E (2003) The influence of the microstructure of hardened tool steel workpiece on the wear of PCBN cutting tools. Int J Machine Tools Manuf 43:139–144
28. Remadna M, Rigal J-F (2006) Evolution during time of tool wear and cutting forces in the case of hard turning with CBN inserts. J Mater Process Technol 178(1–3):67–75
29. Shaw MC (1984) Metal cutting principles. Oxford University Press, Oxford
30. Suresh PVS, Rao PV, Deshmukh SG (2002) A genetic algorithmic approach for optimization of the surface roughness prediction model. Int J Mach Tools Manuf 42:675–680
31. Yallese MA, Boulanouar L, Chaoui K (2004) Usinage de l'acier 100Cr6 trempé par un outil en nitrure de bore cubique. Mécanique Industries 5:355–368
32. Yallese MA, Rigal J-F, Chaoui K, Boulanouar L (2005) The effects of cutting conditions on mixed ceramic and cubic boron nitride tool wear and on surface roughness during machining of X200Cr12 steel (60 HRC). J Eng Manuf 219(B):35–55
33. Yallese MA, Chaoui K, Zeghib N, Boulanouar L, Rigal J-F (2009) Hard machining of hardened bearing steel using cubic boron nitride tool. J Mater Process Technol 209(2009):1092–1104